Semi-analytical numerical procedures for nonlinear differential equations in science and engineering

Modify Andrew Elton Kaunda
Cape Peninsula University of Technology
Jul 2010 - Jan 2022
7 Killarney street
Oakdale
Bellville 7530
South Africa
kaundam@live.com

Abstract

Second order vector-valued nonlinear differential equations occurring in science and engineering have been considered which generally do not have closed-form solutions. Explicit incremental semi-analytical numerical solution procedures for nonlinear multiple-degree-of-freedom systems have been developed. Higher order equivalent differential equations were formulated and then subsequent values of vectors were updated using explicit Taylor series expansions. As the time-step tends to zero, the values of displacement and velocity are exact in the Taylor series expansions involving as many higher order derivatives as necessary. Second order differential equations considered were, the van der Pol equation, Duffing equation and nonlinear equation for the pendulum. A linear second-order two-degrees-of-freedom system subjected to a history of loading, initial conditions of displacement and velocity formed a vector-valued function which was shown to be easily extended to multiple-degrees-of-freedom systems using mass, damping and stiffness matrices such as those obtained from finite element methods. A two-state nonlinear first order differential equation has also been addressed, and the three dimensional system equations derived by Lorenz that demonstrate the phenomenon of chaos. Further applications of the semi-analytical procedures to time-dependent systems should also include, time-independent equations that are differentiable in terms of other independent variables, such as partial differential equations that have many independent variables.

Keywords

Nonlinear dynamical systems; nonlinear oscillatory systems; higher order equivalent differential equations; semi-analytical procedures.

1 Introduction

This article gives details of robust semi-analytical numerical solution procedures for some nonlinear vector-valued (m-dof) first-order, second-order and nth-order differential equations in science and engineering which generally do not have closed-form solutions. Starting by acknowledging the early contributions of the Newmark trapezoidal scheme [1], that possessed limited accuracy and stability characteristics, that was used for time-integration of nonlinear finite element analysis of solids and structures, to further improved solution procedures, such as, the improved numerical dissipation of Hilber et. al. [2], consistent tangent operators of Simo and Taylor [3], time-stepping schemes of Wood [4], simple second order accurate implicit integration schemes of Bathe et. al. [5], and finite element methods of Zienkiewicz et. al. [6].

1.1 Implicit schemes

Zienkiewicz et. al. [6] introduced an implicit generalised Newmark integration scheme from the truncated Taylor series expansion of the displacement function u and its derivatives, as follows

$$\begin{aligned}
u_{n+1} &= u_n + \Delta t \dot{u}_n + ... + \tfrac{\Delta t^p}{p!} u_n^{(p)} + \beta_p \tfrac{\Delta t^p}{p!}(u_{n+1}^{(p)} - u_n^{(p)}) \\
\dot{u}_{n+1} &= \dot{u}_n + \Delta t \ddot{u}_n + ... + \tfrac{\Delta t^{p-1}}{(p-1)!} u_n^{(p)} + \beta_{p-1} \tfrac{\Delta t^{p-1}}{(p-1)!}(u_{n+1}^{(p)} - u_n^{(p)}) \\
&... \\
u_{n+1}^{(p-1)} &= u_n^{(p-1)} + \Delta t u_n^{(p)} + \beta_1 \Delta t (u_{n+1}^{(p)} - u_n^{(p)})
\end{aligned} \tag{1}$$

where $u, \dot{u}, \ddot{u}$, are displacement, velocity and acceleration. Setting $p = 2$ forms the equivalent Newmark scheme [1] which consists of two recurrence equations of displacement and velocity, and when combined with the governing second order differential equation (4), gives three simultaneous equations in three unknowns. Carrying on from these contributions, a forward-backward difference time-integration scheme was developed by Kaunda [7], using Taylor series, for solutions of nonlinear oscillatory systems, giving birth to more accurate implicit generalised one-step multiple-value algorithms [7],[8], repeated here for convenience.

$$s_{n+1} + \sum_{k=1}^{k=p} \frac{(-1)^k}{k!} [\gamma_{1k} \Delta t \frac{d}{dt}]^k s_{n+1} = s^* = s_n + \sum_{k=1}^{k=p} \frac{1}{k!} [\beta_{1k} \Delta t \frac{d}{dt}]^k s_n \tag{2}$$

$$v_{n+1} + \sum_{k=1}^{k=p-1} \frac{(-1)^k}{k!} [\gamma_{2k} \Delta t \frac{d}{dt}]^k v_{n+1} = v^* = v_n + \sum_{k=1}^{k=p-1} \frac{1}{k!} [\beta_{2k} \Delta t \frac{d}{dt}]^k v_n \tag{3}$$

where $s = x$ denotes displacement, $v = \dot{x}$ denotes velocity and $a = \ddot{x}$ represents acceleration. Equations (2) and (3) provide the necessary extra equations to solve the differential equation (4) such that there are

three equations in three unknowns. The implicit algorithms presented in [6],[7],[8], permitted to determine and optimise stability and accuracy of the recurrence equations by choosing appropriate tuneable integration parameters, $\beta_p, \gamma_{ik}, \beta_{ik}$. Numerical dissipation or algorithmic damping, mostly desired in finite element methods, may also be incorporated to filter out high frequency responses, as considered in Hilber et. al. [2].

1.2 Explicit schemes

With supporting literature [6]-[18], on convergence, stability and accuracy, new semi-analytical procedures are now proposed for nonlinear multiple-degree-of-freedom systems with emphasis on reliable explicit incremental solution procedures, as opposed to iterative schemes, which turn out to be fast and accurate and depend on only differentiation (for continuously differentiable functions), as opposed to integration (usually difficult for nonlinear equations), to solve nonlinear differential equations. As a result, stability of the algorithms is conditional and for small increments, convergence, stability and accuracy are simultaneously achieved. The explicit algorithm being focused in this paper is a subset of the implicit algorithms given by equations (1), (2) and (3), where $\beta_p = 0, \gamma_{ik} = 0, \beta_{ik} = 1$. Semi-analytical methods for the n-th order governing differential equations use higher order equivalent differential equations. For example, the second order differential equation (4), only displacement and velocity recurrence equations (2) and (3), which are associated with prescribed initial conditions, are updated using Taylor series.

The article is organised as follows: Section 2 develops the solution of nonlinear vector-valued oscillatory systems. Section 3 develops a two-degrees-of-freedom system, nonlinear two-state first order differential equations and extension to multiple-degree-of-freedom systems using mass, damping and stiffness matrices such as those obtained from finite element methods. Section 4 presents and discusses results, and Section 5 draws conclusions.

2 Nonlinear vector-valued oscillatory system

The differential equation describing a nonlinear vector-valued oscillatory system may have the general form

$$\ddot{x} + f(\dot{x}, x, t) = 0; x(0) = x_0; \dot{x}(0) = \dot{x}_0; t = t_0 \tag{4}$$

The superposed dot on x, represents differentiation with respect to time, t, and double-dot represents second derivative. Closed-form solutions of most nonlinear systems do not exist.

2.1 Van der Pol equation

The van der Pol equation, which fits in the general case of equation (4), is described by the single-valued differential equation (5), which is an example of soft nonlinear systems. The stable oscillations, also called relaxation oscillations are a type of limit cycle in electrical circuits employing vacuum tubes. Attention is drawn to an autonomous system where the time, t, is not an explicit variable.

$$\ddot{x} + \mu(x^2 - 1)\dot{x} + x = 0; x(0) = x_0; \dot{x}(0) = \dot{x}_0; \mu > 0 \tag{5}$$

which may be written as

$$\ddot{x} - \mu\dot{x} + x = -\mu\dot{x}x^2 = -\mu\frac{d}{dt}(\frac{1}{3}x^3) \tag{6}$$

where μ, is a positive constant. Equation (5) represents a differential equation with variable damping, and for $|x| > 1$ possesses a unique limit cycle, δ, which must surround the origin [13]. The earliest work on this relaxation oscillator started by Appleton [19] and van der Pol [20], but various Russian authors had given very general methods of establishing the existence of periodic, or almost periodic, solutions of a class of equations which includes the van der Pol equation. These methods usually involved transforming the equation into a pair of equations, and a good deal of manipulation; the methods depended on the general theory of differential equations including the Poincare theory of solutions in powers of a small parameter. Cartwright and co-workers, [21],[22],[23], dedicated their mathematical skills in solving the van der Pol system equations. However, a closed-form solution remains elusive for $\mu >> 0$, and this is the motivation for the present article.

Marios Tsatsos [24] conducted a theoretical and numerical study of the van der Pol equation in a thesis and presented some theory of averaging, successive approximations and symbolic dynamics. A historical outline was given regarding modern applications and modelling with the van der Pol oscillator, from experiments with oscillations in a vacuum tube triode circuit such that all initial conditions converged to the same periodic orbit of finite amplitude, to models concerning a variety of physical and biological phenomena, such as stability of the human heart dynamics.

A very comprehensive historical paper was published in 2016 by Jean-Marc Ginoux [25]. It gives details of the development of state of the art work, from nonlinear oscillations to chaos theory. No closed-form or general analytical solution of the van der Pol equation exists, which is the motivation for the current numerical contributions. Some graphical and limited methods of solution are given in Strogatz [12] and Jordan et. al. [17], who also cite numerous examples such as: the beating of a heart; the periodic firing of a pacemaker neuron; daily rhythms in human body temperature and hormone secretion; chemical reactions that oscillate spontaneously; and dangerous self-excited vibrations in bridges and aeroplane wings. The period, waveform and amplitude of oscillations are looked at in each of these examples. In this article, simple and robust semi-analytical solution methods are considered.

2.1.1 Natural frequency and period of oscillation

It is observed, see Figure 2, that, as $\mu \to +\infty$, there is a positive infinite slope in displacement, x, in the interval $-1 \leq x \leq +2$ and a negative infinite slope in displacement in the interval $+1 \geq x \geq -2$, and the velocity is practically, $\dot{x} << \dot{x}_{max}$, during the displacement intervals, $-2 \leq x \leq -1$ and $+2 \geq x \geq +1$ proceeding in a clock-wise phase trajectory.

The period of oscillation for the van der Pol equation is derived from observing the displacement - time graph of Figure 2, and the velocity - displacement graph of Figure 3. For $\mu >> 1$, and choosing displacement, $x_1 = 2$, corresponding to time, $t_1 = \tau/2$, and next displacement $x_2 = 1$, corresponding to $t_2 = \tau$, with corresponding velocities, such that $(\dot{x}_2 - \dot{x}_1) << \mu\frac{4}{3}$, as shown in Table 1. By integration over the time interval, dt

$$\begin{array}{l} \ddot{x} + \mu(x^2 - 1)\dot{x} + x = 0 \\ \int \ddot{x}dt + \int \mu(x^2 - 1)\dot{x}dt + \int xdt = 0 \end{array} \tag{7}$$

Recall

$$\ddot{x}dt = d\dot{x}, \dot{x}dt = dx, x_{ave} = (x_1 + x_2)/2 = \frac{3}{2} \tag{8}$$

Then

$$\begin{array}{l} \int d\dot{x} + \int \mu(x^2 - 1)dx + x_{ave}\int dt = 0 \\ \dot{x} + \mu(\frac{x^3}{3} - x) + x_{ave}t + C = 0 \;\; Indefinite \;\; integral \\ \dot{x}|_{\dot{x}_1}^{\dot{x}_2} + \mu(\frac{x^3}{3} - x)|_{x_1}^{x_2} + \frac{3}{2}t|_{t_1}^{t_2} = 0 \;\; Definite \;\; integral \\ (\dot{x}_2 - \dot{x}_1) - \mu\frac{4}{3} + \frac{3}{4}\tau = 0 \\ \tau = \mu\frac{16}{9} \\ \omega = \frac{1}{\mu}\frac{9\pi}{8} \end{array} \tag{9}$$

where $\int_{\tau/2}^{\tau} cdt$ was used to represent an average value, $c = x_{ave}$. Rewriting the van der Pol equation and integrating,

$$\begin{array}{l} \ddot{x} + \mu(x^2 - 1)\dot{x} + x = 0 \\ \int \ddot{x}dt + \int \mu(x^2 - 1)\dot{x}dt + \int xdt = 0 \\ \int d\dot{x} + \int \mu(x^2 - 1)dx + \int xdt = 0 \end{array} \tag{10}$$

If $\int d\dot{x} = (\dot{x}_2 - \dot{x}_1) = 0$, as is the case at (x_1, x_2), then the last equation is approximated by

$$\int \mu(x^2 - 1)dx + \int xdt \approx 0 \tag{11}$$

Dividing through by x,

$$\int \mu\frac{(x^2 - 1)}{x}dx + \int dt \approx 0 \tag{12}$$

and integrating over $(x_1 = 2, x_2 = 1)$ and $(t_1 = \tau/2, t_2 = \tau)$, yields $\tau = \mu(3 - 2ln2)$. For $\mu >> 1$, the value of period, $\tau = \mu\frac{16}{9}$, given by equation (9), compares favourably with $\tau = \mu(3 - 2ln2) + 2\alpha\mu^{-0.333} + ...$, where $\alpha = 2.338$, as derived in Strogatz [12], and the corresponding natural frequency is $\omega = \frac{1}{\mu}\frac{9\pi}{8}$.

2.1.2 Maximum velocity and point of inflexion

At $t = \tau$, the equation for maximum velocity is now derived by integration over the time interval, dt.

$$\begin{array}{l} \ddot{x} + \mu(x^2 - 1)\dot{x} + x = 0 \\ \int \ddot{x}dt + \int \mu(x^2 - 1)\dot{x}dt + \int xdt = 0 \\ \int d\dot{x} + \int \mu(x^2 - 1)dx + x_{ave}\int dt = 0 \\ \dot{x}|_0^{\dot{x}_{max}} + \mu(\frac{x^3}{3} - x)|_{-2}^{-1} + \frac{3}{2}t|_{\tau}^{\tau} = 0 \\ \dot{x}_{max} = -\frac{4}{3}\mu \;\; or \;\; |\dot{x}_{max}| = \frac{4}{3}\mu \end{array} \tag{13}$$

Table 1: Relationships between displacement, velocity and acceleration for $\mu = 160$

t	x_t	$\dot{x}_a$	$\ddot{x}_a$	$\dot{x}_b$	$\ddot{x}_b$
$\tau/2$	2.0	0	-2	-213.3333	1.0240e+05
$\approx 3\tau/4$	1.5000	120	-2.4002e+04	0	-1.5000
$\approx \tau$	1.2500	191.6703	-1.7252e+04	-0.0036	-0.9272
τ	1	213.3333	-1	0	-1
τ	0.7500	195.0022	1.3649e+04	-0.0022	-0.9070
τ	0.5000	146.6667	1.7600e+04	0	-0.5000
τ	0.2500	78.3357	1.1750e+04	-0.0024	-0.6090
τ	0	0.5000	80	-0.5000	-6.4382
τ	-0.2500	0.0024	0.6090	-78.3357	-1.1750e+04
τ	-0.5000	0	0.5000	-146.6667	-1.7600e+04
τ	-0.7500	-0.0016	0.6378	-194.9984	-1.3649e+04
τ	-1	-0.0035	1	-213.3298	1
τ	-1.2500	-0.0068	1.8663	-191.6598	1.7251e+04
τ	-1.5000	-0.0167	4.8338	-119.9833	2.3998e+04
τ	-1.7500	11.4204	-3.7670e+03	0.2463	-79.5191
τ	-2	213.3158	-1.0239e+05	0.0176	-6.4382

Note:
$\tau/2 \le t \le \tau$
$\ddot{x} + \mu(x^2 - 1)\dot{x} + x = 0$
$\frac{\dot{x}^2}{2} + \mu(\frac{x^3}{3} - x)\dot{x} + \frac{x^2}{2} + C = 0$
$x = x_0, \dot{x} = \dot{x}_0, C = -[\frac{\dot{x}_0^2}{2} + \mu(\frac{x_0^3}{3} - x_0)\dot{x}_0 + \frac{x_0^2}{2}]$
Solve for quadratic in $\dot{x}$ given any $-2 < x_t < 2$, see Figure 5
$\mu\frac{x^3}{3}\dot{x} + \frac{x^2}{2} - \mu x\dot{x} + \frac{\dot{x}^2}{2} + C = 0$
Solve for cubic in x given any $-\mu\frac{4}{3} < \dot{x}_t < \mu\frac{4}{3}$, see Figures 6, 7
$\ddot{x} = f(\dot{x}, x)$; $\dot{x} = f(x)$,
From the table,
$x_{max} = 2$,
$\dot{x}_{max} = 213.3333 \;\; at \;\; x = 1 \;\; or \;\; x = -1$,
$\ddot{x}_{large} = 1.0239e + 05 > \ddot{x}_{max} \;\; when \;\; x = x_{max}$ outside limit cycle
$(\dot{x}_2 - \dot{x}_1) = (\dot{x}_{x=0} - \dot{x}_{x=2}) = (0.5000 - 0) = 0.5000$
$\tau = [\frac{4}{3}\mu - (\dot{x}_2 - \dot{x}_1)]/\frac{3}{4} = [\frac{16}{9}\mu - \frac{4}{3}(\dot{x}_2 - \dot{x}_1)] \approx \frac{16}{9}\mu$
$\omega = 2\pi/\tau$

From Figure 3, this is the interval, $-1 \ge x \ge -2$, where x drops down steeply with $t_1 \approx t_2 = \tau$ in a clockwise phase trajectory. The relationship between τ and $\dot{x}_{max}$ is, $\mu = \tau\frac{9}{16} = \dot{x}_{max}\frac{3}{4}$, which gives $\dot{x}_{max} = \tau\frac{3}{4} = \frac{2\pi}{\omega}\frac{3}{4} = \Omega$. Within the interval $0.5 \ge x \ge -0.5$, there is a point of inflexion for velocity, see Figures 3 and 10, given by

$$\begin{aligned} &\ddot{x} + \mu(x^2 - 1)\dot{x} + x = 0 \\ &\int \ddot{x}dt + \int \mu(x^2 - 1)\dot{x}dt + \int xdt = 0 \\ &\int d\dot{x} + \int \mu(x^2 - 1)dx + x_{ave}\int dt = 0 \\ &\dot{x}|_0^{\dot{x}_{inf}} + \mu(\frac{x^3}{3} - x)|_{0.5}^{-0.5} + \frac{3}{2}t|_{\tau}^{\tau} = 0 \\ &\dot{x}_{inf} = -\frac{275}{300}\mu \;\; or \;\; |\dot{x}_{inf}| = \frac{275}{300}\mu \end{aligned} \tag{14}$$

This means that for a given value of μ, the inflexion point of velocity is $|\dot{x}_{inf}| = \frac{275}{300}\mu$, as seen on a plot of velocity $\dot{x}$ vs displacement x. Alternatively, by integration over dx

$$\begin{aligned} &\ddot{x} + \mu(x^2 - 1)\dot{x} + x = 0 \\ &\int \ddot{x}dx + \int \mu\frac{d}{dt}(\frac{x^3}{3} - x)dx + \int xdx = 0 \\ &\int \dot{x}d\dot{x} + \frac{d}{dt}\int \mu(\frac{x^3}{3} - x)dx + \int xdx = 0 \\ &\int \dot{x}d\dot{x} + \frac{d}{dt}\mu(\frac{x^4}{12} - \frac{x^2}{2}) + \int xdx = 0 \\ &\frac{\dot{x}^2}{2}|_0^{\dot{x}_{max}} + \mu(\frac{x^3}{3} - x)\dot{x}|_{(-2,0)}^{(-1,\dot{x}_{max})} + \frac{x^2}{2}|_{-2}^{-1} = 0 \\ &\dot{x}_{max} = 0, \;\; \dot{x}_{max} = -\frac{4}{3}\mu \;\; or \;\; |\dot{x}_{max}| = \frac{4}{3}\mu \;\; for \;\; \mu >> 1 \end{aligned} \tag{15}$$

One half-cycle of the van der Pol oscillator consists of intervals, $2 \geq x \geq 1$, $1 \geq x \geq -1$, and $-1 \geq x \geq -2$ in a clockwise phase trajectory. The last interval is now considered by integration over dx.

$$\begin{array}{l} \ddot{x} + \mu(x^2 - 1)\dot{x} + x = 0 \\ \int \ddot{x}dx + \int \mu \frac{d}{dt}(\frac{x^3}{3} - x)dx + \int xdx = 0 \\ \int \dot{x}d\dot{x} + \frac{d}{dt}\int \mu(\frac{x^3}{3} - x)dx + \int xdx = 0 \\ \int \dot{x}d\dot{x} + \frac{d}{dt}\mu(\frac{x^4}{12} - \frac{x^2}{2}) + \int xdx = 0 \\ \frac{\dot{x}^2}{2} + \mu(\frac{x^3}{3} - x)\dot{x} + \frac{x^2}{2} + C = 0 \quad (Indefinite \;\; integral) \\ \frac{\dot{x}^2}{2}|_{\dot{x}_{max}}^{0} + \mu(\frac{x^3}{3} - x)\dot{x}|_{(-1,\dot{x}_{max})}^{(-2,0)} + \frac{x^2}{2}|_{-1}^{-2} = 0 \quad (Definite \;\; integral) \\ \dot{x}_{max} = 0, \;\; \dot{x}_{max} = -\frac{4}{3}\mu \;\; for \;\; \mu >> 1 \end{array} \tag{16}$$

Again, the maximum velocity is, $\dot{x}_{max} = \frac{4}{3}\mu$.

2.1.3 Maximum acceleration and point of inflexion

Given the acceleration in the form

$$\ddot{x} = -(\mu(x^2 - 1)\dot{x} + x) \tag{17}$$

the acceleration, $\ddot{x} = 0$, when $(\dot{x} = x = 0)$. The maximum acceleration, $\ddot{x} = \ddot{x}_{max}$, is approximately when $(x = -1.6, x = -0.4, x = 0.4, x = 1.6)$ and $(\dot{x} = \dot{x}_{inf}, \dot{x} = -\dot{x}_{inf})$. Acceleration has a point of inflexion, $\ddot{x} = \ddot{x}_{inf}$, when approximately $(-0.25 \leq x \leq 0.25)$, see Figure 4, specifically for which $\dot{x}_{inf} = \mu\frac{29375}{60000}$. The maximum acceleration is found by differentiating acceleration with respect to displacement and velocity and equating the result to zero for maxima or minima or point of inflexion.

$$\begin{array}{l} \frac{d}{d\dot{x}}(\ddot{x}) = -\mu(x^2 - 1) \\ \frac{d}{dx}(\ddot{x}) = -(\mu(2x)\dot{x} + 1) \end{array} \tag{18}$$

such that $(\frac{d\ddot{x}}{dx} + \frac{d\ddot{x}}{d\dot{x}}) = 0$, or

$$-\mu(x^2 - 1) - (\mu(2x)\dot{x} + 1) = 0 \tag{19}$$

Recall that

$$\begin{array}{l} \dot{x} = \frac{dx}{dt}; \quad \ddot{x} = \frac{d\dot{x}}{dt}; \quad \dddot{x} = \frac{d\ddot{x}}{dt} \\ dt = \frac{dx}{\dot{x}} = \frac{d\dot{x}}{\ddot{x}} = \frac{d\ddot{x}}{\dddot{x}} \\ \frac{d\ddot{x}}{dx} = \frac{\dddot{x}}{\dot{x}} = -(\mu(2x)\dot{x} + 1) \quad and \quad \frac{d\ddot{x}}{d\dot{x}} = \frac{\dddot{x}}{\ddot{x}} = -\mu(x^2 - 1) \end{array} \tag{20}$$

Therefore, the time-derivative of acceleration, $\dddot{x} = 0$, since $(\frac{d\ddot{x}}{dx} + \frac{d\ddot{x}}{d\dot{x}}) = (\frac{\dddot{x}}{\dot{x}} + \frac{\dddot{x}}{\ddot{x}}) = 0$, it follows that

$$\dddot{x} = -[\mu(x^2 - 1)\ddot{x} + (2\mu x\dot{x} + 1)\dot{x}] = 0$$

$$\begin{array}{l} \ddot{x}_{max} = -\frac{(2\mu x\dot{x}+1)\dot{x}}{\mu(x^2-1)}; \quad x \neq 1; \\ \quad \ddddot{x} > 0 \;\; for \;\; \ddot{x} = \ddot{x}_{min}; \\ \quad \ddddot{x} < 0 \;\; for \;\; \ddot{x} = \ddot{x}_{max}; \\ \quad \dddddot{x} = -[(\mu(6x\dot{x}) + 1)\ddot{x} + \mu 2\dot{x}^3] = 0 \;\; for \;\; \ddot{x} = \ddot{x}_{inf} \\ \ddot{x}_{inf} = -\frac{2\mu\dot{x}^3}{1+6\mu x\dot{x}} \end{array} \tag{21}$$

For $\mu = 160$, the approximate observed local maxima of acceleration in one periodic cycle are shown in Table 2. It is observed that there is a point of asymptotes between the times 0.08200 and 0.08900 *seconds* where the acceleration peaks at -17955.6 then suddenly jumps to 27701.7 (m/s^2). This is also observed between the times 112.650 and 112.657 (0.4τ) *seconds* as well as between the times 242.378 and 242.384 (0.85τ) *seconds*. This is confirmed in the graph of acceleration vs time in Figure 8.

Table 2: Maximum acceleration

t	x	$\dot{x}$	$\ddot{x}$
0.08200	-0.590700	-156.887	-17955.6
0.08900	-1.675090	-90.6957	27701.7
112.650	0.547982	186.977	22587.4
112.657	1.786850	88.6905	-35829.3
242.378	-0.441346	-173.106	-22301.6
242.384	-1.728500	-108.201	36126.8

The second order differential equation of the van der Pol oscillator may be recast as

$$\ddot{x} = f(\dot{x}, x, t) = -[\mu(x^2 - 1)\dot{x} + x] \tag{22}$$

After differentiating the equation with respect to time

$$\begin{aligned}
\dddot{x} &= -[\mu(x^2-1)\ddot{x} + \mu(2x\dot{x})\dot{x} + \dot{x}] \\
\ddddot{x} &= -[\mu(x^2-1)\,\dddot{x} + \mu(2x\dot{x})\ddot{x} \\
&\quad + \mu 2(x\dot{x})\ddot{x} + \mu 2(\dot{x}^2 + x\ddot{x})\dot{x} + \ddot{x}] \\
x^{(5)} &= -[\mu(x^2-1)\,\ddddot{x} + \mu(2x\dot{x})\,\dddot{x} \\
&\quad + \mu 2(x\dot{x})\,\dddot{x} + \mu 2(\dot{x}^2 + x\ddot{x})\ddot{x} \\
&\quad + \mu 2(x\dot{x})\,\dddot{x} + \mu 2(\dot{x}^2 + x\ddot{x})\ddot{x} \\
&\quad + \mu 2(\dot{x}^2 + x\ddot{x})\ddot{x} + \mu 2(2\dot{x}\ddot{x} + \ddot{x}^2 + x\,\dddot{x})\dot{x} + \ddddot{x}] \\
&\ldots \\
x^{(N)} &= \tfrac{d^{N-2}}{dt^{N-2}} f(\dot{x}, x, t)
\end{aligned} \tag{23}$$

These derivatives have been obtained analytically, which will be used in the solution of the waveform of the van der Pol oscillator, using the semi-analytical procedures considered in Section 2.4.

2.2 Duffing oscillator

The Duffing equation is given by a nonlinear second order differential equation (24)

$$\ddot{x} + \delta\dot{x} + \alpha x + \beta x^3 = \gamma cos(\omega t); x(0) = x_0, \dot{x}(0) = \dot{x}_0 \tag{24}$$

where x, is the displacement, $\dot{x}$, velocity, $\ddot{x}$, acceleration, and $\delta, \alpha, \beta, \gamma, \omega$ are constants. Such systems occur in vibration of mechanical systems with nonlinear restoring forces, such as soft and hard nonlinear springs, which do not obey Hooke's law. The second order differential equation may be recast as

$$\ddot{x} = f(\dot{x}, x, t) = \gamma cos(\omega t) - [\delta\dot{x} + \alpha x + \beta x^3] \tag{25}$$

After differentiating the equation with respect to time

$$\begin{aligned}
\dddot{x} &= -\gamma\omega sin(\omega t) - [\delta\ddot{x} + \alpha\dot{x} + 3\beta x^2\dot{x}] \\
\ddddot{x} &= -\gamma\omega^2 cos(\omega t) - [\delta\,\dddot{x} + \alpha\ddot{x} + 3\beta(2x\dot{x}^2 + x^2\ddot{x})] \\
x^{(5)} &= \gamma\omega^3 sin(\omega t) - [\delta\,\ddddot{x} + \alpha\,\dddot{x} + 3\beta[2(\dot{x}^3 + x2\dot{x}\ddot{x}) + 2x\dot{x}\ddot{x} + x^2\,\dddot{x}]] \\
x^{(6)} &= \gamma\omega^4 cos(\omega t) - [\delta x^{(5)} + \alpha\,\ddddot{x} + 3\beta[2(3\dot{x}^2\ddot{x} + 2(\dot{x}^2 + x\ddot{x}^2 + x\dot{x}\,\dddot{x})) \\
&\quad + 2(\dot{x}^2 + x\ddot{x}^2 + x\dot{x}\,\dddot{x}) + 2x\dot{x}\,\dddot{x} + x^2\,\ddddot{x}]] \\
&\ldots \\
x^{(N)} &= \tfrac{d^{N-2}}{dt^{N-2}} f(\dot{x}, x, t)
\end{aligned} \tag{26}$$

These derivatives have been obtained analytically, which will be used in the solution of the waveform of the Duffing oscillator, using the semi-analytical procedures considered in Section 2.4.

2.3 Pendulum

A nonlinear equation of a simple pendulum oscillating about an equilibrium position is of the form

$$\ddot{\theta} + \frac{g}{L} sin(\theta) = 0 \tag{27}$$

where g, is the acceleration due gravity, and θ, is the angular deflection from equilibrium of the pendulum of length, L. The second order differential equation may be recast as

$$\ddot{\theta} = f(\theta) = -\frac{g}{L} sin(\theta) \tag{28}$$

After differentiating the equation with respect to time

$$\begin{aligned}
\dddot{\theta} &= -\tfrac{g}{L}\dot{\theta} cos(\theta) \\
\ddddot{\theta} &= -\tfrac{g}{L}[\ddot{\theta} cos(\theta) - \dot{\theta}^2 sin(\theta)] \\
\theta^{(5)} &= -\tfrac{g}{L}[(\,\dddot{\theta} cos(\theta) - \dot{\theta}\ddot{\theta} sin(\theta)) \\
&\quad - (2\dot{\theta}\ddot{\theta} sin(\theta) + \dot{\theta}^3 cos(\theta))] \\
&\ldots \\
x^{(N)} &= \tfrac{d^{N-2}}{dt^{N-2}} f(\theta)
\end{aligned} \tag{29}$$

These derivatives have been obtained analytically, which will be used in the solution of the waveform of the nonlinear pendulum swing, using the semi-analytical procedures considered in Section 2.4.

2.4 Semi-analytical procedures for nonlinear vector-valued differential equations

For each of the above equations, in general homogeneous or non-homogeneous forms, the solution procedure is carried out as follows

$$\begin{array}{l}\ddot{x} = f(\dot{x}, x, t), \quad for \quad x(0) = x_0, \dot{x}(0) = \dot{x}_0 \\ \dddot{x} = \frac{d}{dt} f(\dot{x}, x, t) = \dot{f}(\ddot{x}, \dot{x}, x, t) \\ \ddddot{x} = \frac{d^2}{dt^2} f(\dot{x}, x, t) = \ddot{f}(\dddot{x}, \ddot{x}, \dot{x}, x, t) \\ x^{(5)} = \frac{d^3}{dt^3} f(\dot{x}, x, t) = \dddot{f}(\ddddot{x}, \dddot{x}, \ddot{x}, \dot{x}, x, t) \\ ... \\ x^{(N)} = \frac{d^{N-2}}{dt^{N-2}} f(\dot{x}, x, t)\end{array} \tag{30}$$

These form higher-order equivalent differential equations [9] which are used in the solution of the waveform of the nonlinear vectors. Further higher order derivatives may be necessary to increase accuracy, for $N \to \infty$. For the implicit iterative algorithms involving higher order derivatives exceeding the order of the differential equation, initial conditions of the vectors are determined at the beginning of each iteration, where the higher order equivalent differential equations come in handy. In contrast, for explicit algorithms, subsequent vector values of displacements, x_i, and velocities, $\dot{x}_i$, are determined and updated recursively from the explicit Taylor series expansions

$$\begin{array}{l}x_{n+1} = x_n + \Delta t \dot{x}_n + \frac{\Delta t^2}{2!} \ddot{x}_n + \frac{\Delta t^3}{3!} \dddot{x}_n + ..., n = 0, 1, 2, 3, ... \\ \dot{x}_{n+1} = \dot{x}_n + \Delta t \ddot{x}_n + \frac{\Delta t^2}{2!} \dddot{x}_n + \frac{\Delta t^3}{3!} \ddddot{x}_n + ..., n = 0, 1, 2, 3, ...\end{array} \tag{31}$$

where the analytically obtained acceleration and higher-order derivatives are evaluated from the higher order equivalent differential equations. This is the first time in the procedure where errors are committed in the algorithm because of terminating the Taylor series at an upper summation limit of $N \ll \infty$. Then, for each of the above equations, the solution procedure recursively proceeds as follows

$$\begin{array}{l}\ddot{x} = f(\dot{x}, x, t), \quad for \quad x(n) = x_n, \dot{x}(n) = \dot{x}_n, \quad n = 0, 1, 2, 3, .. \\ ... \\ x^{(N)} = \frac{d^{N-2}}{dt^{N-2}} f(\dot{x}, x, t)\end{array} \tag{32}$$

where the new accepted sub-initial conditions are $x(n) = x_n, \dot{x}(n) = \dot{x}_n, \quad n = 1, 2, 3, ...$ Note that finite difference methods, such as central difference or backward difference or implicit schemes, are not used in the above algorithm. The procedure is therefore an explicit incremental forward difference method using the Taylor series updates. Clearly, as the time-step, $\Delta t \to 0$, the values of displacement and velocity are exact in the Taylor series expansions involving as many higher order derivatives as necessary, for $N \to \infty$. The explicit algorithm convergence, stability, accuracy and speed depend on the size of the time-step and number of higher-order derivatives included. For most practical examples, this is not a set back when compared with implicit algorithms. The convergence may be tested using the ratio test for both the displacement and velocity Taylor series which have to be updated. The stability is conditional depending on the size of the time-step.

2.4.1 Practical termination of and error in recurrence equations

Ideally, the recurrence equations should be terminated at $N \to \infty$. Practically, for most accurate results

$$\begin{array}{l}x_{n+1} = x_n + \Delta t \dot{x}_n + \frac{\Delta t^2}{2!} \ddot{x}_n + \frac{\Delta t^3}{3!} \dddot{x}_n + ..., + \frac{\Delta t^N}{N!} x_{\zeta_s}^{(N)} \quad n < \zeta_s = n(1 + \frac{1}{N+1}) < n + 1 \\ \quad n = 0, 1, 2, 3, ... \\ \dot{x}_{n+1} = \dot{x}_n + \Delta t \ddot{x}_n + \frac{\Delta t^2}{2!} \dddot{x}_n + \frac{\Delta t^3}{3!} \ddddot{x}_n + ... + \frac{\Delta t^{N-1}}{(N-1)!} x_{\zeta_v}^{(N)} \quad n < \zeta_v = n(1 + \frac{1}{N}) < n + 1 \\ \quad n = 0, 1, 2, 3, ...\end{array} \tag{33}$$

where $n < \zeta_s = n(1+\frac{1}{N+1}) < n+1$ represents the point where the last term is evaluated, at time, $t_n < t_{\zeta_s} < t_{n+1}$, for the displacement, x_n, and $n < \zeta_v = n(1 + \frac{1}{N}) < n + 1$, at time, $t_n < t_{\zeta_v} < t_{n+1}$, for the velocity, $\dot{x}_n$ and N is the highest power of Δt for each series, respectively. The best estimate for $\zeta = n(1 + \frac{1}{N})$ is elegantly derived in Irons et. al. [14]. The errors for displacement and velocity recurrence equations are, respectively, of order $O(\frac{\Delta t^N}{N!} x_{\zeta_s}^{(N)})$ and $O(\frac{\Delta t^{N-1}}{(N-1)!} x_{\zeta_v}^{(N)})$.

2.4.2 Radius of convergence

The mathematical ratio test may be defined [18] for a power series centered at $x = a$ by the radius of convergence

$$\lim_{n \to \infty} R = \frac{|C_n|}{|C_{n+1}|} \tag{34}$$

In this article, the following algorithm was adopted:

$$\begin{aligned} \lim_{n\to\infty} R_1 &= \frac{|C_{n-1}|}{|C_n|} \\ \lim_{n\to\infty} R_2 &= \frac{|C_{n-2}|}{|C_{n-1}|} \\ \lim_{n\to\infty} R_3 &= \frac{|C_{n-3}|}{|C_{n-2}|} \end{aligned} \tag{35}$$

Then, the radius of convergence adopted was, $R = min(R, R_1, R_2, R_3)$, where $C_n = \frac{f^{(n)}}{n!}$ and $C_{n+1} = \frac{f^{(n+1)}}{(n+1)!}$ and $f^{(n)} = x^{(n)} = \frac{dx^n}{dt^n}$ from the Taylor series given above.

1. If $R = \infty$, then the series converges for all x
2. If $0 < R < \infty$, then the series converges for all $|x - a| < R$
3. If $R = 0$, then the series converges only for $x = a$

The ratio test needs to be done for both the displacement and velocity Taylor series, for the purpose of adjusting the size of time increments, for example, monitoring that the increment, $\Delta t < R$. If the time step is prescribed at the beginning of the algorithm such that $\Delta t \geq R$, the ratio test could be applied to adjust the time-step appropriately, especially in the first time increment. Repeating the ratio test after every time-step may increase the overall execution time and cost of the algorithm. A similar adaptive time stepping has been considered and presented in Y. Wang et. al. [26].

3 Vector-valued differential functionals

3.1 Two-degrees-of-freedom systems (2-dof)

A linear second-order two-degrees-of-freedom system subjected to a history of loading $f_i(t)$, initial conditions of displacement $x_i(0)$, and velocity $\dot{x}_i(0)$ forms a vector-valued function, and is shown in Figure 1.

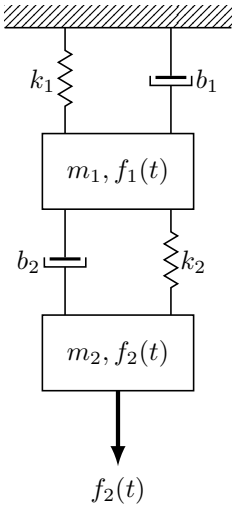

Figure 1: 2-dof: Mass-spring-damper system

$$\begin{bmatrix} m_{11} & m_{12} \\ m_{21} & m_{22} \end{bmatrix} \begin{Bmatrix} \ddot{x}_1 \\ \ddot{x}_2 \end{Bmatrix} + \begin{bmatrix} b_{11} & b_{12} \\ b_{21} & b_{22} \end{bmatrix} \begin{Bmatrix} \dot{x}_1 \\ \dot{x}_2 \end{Bmatrix} + \begin{bmatrix} k_{11} & k_{12} \\ k_{21} & k_{22} \end{bmatrix} \begin{Bmatrix} x_1 \\ x_2 \end{Bmatrix} = \begin{Bmatrix} f_1 \\ f_2 \end{Bmatrix} \tag{36}$$

which is differentiated once with respect to time to get a third-order differential equation, and so on, to form higher-order equivalent differential equations [9].

$$\begin{bmatrix} m_{11} & m_{12} \\ m_{21} & m_{22} \end{bmatrix} \begin{Bmatrix} \dddot{x}_1 \\ \dddot{x}_2 \end{Bmatrix} + \begin{bmatrix} b_{11} & b_{12} \\ b_{21} & b_{22} \end{bmatrix} \begin{Bmatrix} \ddot{x}_1 \\ \ddot{x}_2 \end{Bmatrix} + \begin{bmatrix} k_{11} & k_{12} \\ k_{21} & k_{22} \end{bmatrix} \begin{Bmatrix} \dot{x}_1 \\ \dot{x}_2 \end{Bmatrix} = \begin{Bmatrix} \dot{f}_1 \\ \dot{f}_2 \end{Bmatrix} \tag{37}$$

After differentiating the third-order differential equation with respect to time a fourth-oder system is obtained

$$\begin{bmatrix} m_{11} & m_{12} \\ m_{21} & m_{22} \end{bmatrix} \begin{Bmatrix} \ddddot{x}_1 \\ \ddddot{x}_2 \end{Bmatrix} + \begin{bmatrix} b_{11} & b_{12} \\ b_{21} & b_{22} \end{bmatrix} \begin{Bmatrix} \dddot{x}_1 \\ \dddot{x}_2 \end{Bmatrix} + \begin{bmatrix} k_{11} & k_{12} \\ k_{21} & k_{22} \end{bmatrix} \begin{Bmatrix} \ddot{x}_1 \\ \ddot{x}_2 \end{Bmatrix} = \begin{Bmatrix} \ddot{f}_1 \\ \ddot{f}_2 \end{Bmatrix} \tag{38}$$

These form higher order equivalent differential equations [9] which are used in the solution of the waveform of the nonlinear vectors, using the semi-analytical procedures considered in Section 2.4. Further higher order derivatives may be neccessary to increase accuracy. The eigenvalues λ, are determined from the eigenvalue problem or eigenproblem

$$Av = \lambda v \tag{39}$$

where

$$A = \begin{bmatrix} m_{11} & m_{12} \\ m_{21} & m_{22} \end{bmatrix}^{-1} \begin{bmatrix} k_{11} & k_{12} \\ k_{21} & k_{22} \end{bmatrix} \tag{40}$$

and the corresponding natural frequencies are $\omega_i = \lambda_i^{\frac{1}{2}}$, and v is the eigenvector of the eigenproblem. Vector values of displacements, x_i, and velocities, $\dot{x}_i$, are then determined and updated recursively from the explicit Taylor series expansions

$$\begin{array}{l} x_{n+1} = x_n + \Delta t \dot{x}_n + \frac{\Delta t^2}{2!}\ddot{x}_n + \frac{\Delta t^3}{3!}\dddot{x}_n + ..., n = 0, 1, 2, 3, ... \\ \dot{x}_{n+1} = \dot{x}_n + \Delta t \ddot{x}_n + \frac{\Delta t^2}{2!}\dddot{x}_n + \frac{\Delta t^3}{3!}\ddddot{x}_n + ..., n = 0, 1, 2, 3, ... \end{array} \tag{41}$$

where the exact vector values of acceleration and higher-order derivatives are evaluated from the higher-order equivalent differential equations.

3.2 Multiple-degrees-of-freedom systems (m-dof)

Vector-valued functions can be handled easily using matrices and vectors, such as mass matrices, M, damping matrices, B, and stiffness matrices, K, for example, obtained from finite-element methods so that

$$[M]\{a\} + [B]\{v\} + [K]\{s\} = \{f\} \tag{42}$$

where $\{a\}, \{v\}, \{s\}, \{f\})$, are acceleration, velocity, displacement, and force vectors, respectively, and where the exact values of higher-order derivatives are evaluated analytically from the higher order equivalent differential equations.

3.3 Nonlinear first-order system state equations (1-dof)

Consider a first-order system of differential equations, a nonlinear two-degrees-of-freedom system taken from Meirovitch [15], subject to initial conditions of displacements $x_i(0)$

$$\begin{array}{l} \dot{x}_1 = x_2 + x_1(1 - x_1^2 - x_2^2) \\ \dot{x}_2 = -x_1 + x_2(1 - x_1^2 - x_2^2) \end{array} \tag{43}$$

The velocities $\dot{x}_i$, are obtained from the initial conditions x_1, x_2, given above. By differentiating the velocities with respect to time, the accelerations, $\ddot{x}_i$ are then obtained as follows:

$$\begin{array}{l} \ddot{x}_1 = \dot{x}_2 + \dot{x}_1(1 - x_1^2 - x_2^2) + x_1(-2x_1\dot{x}_1 - 2x_2\dot{x}_2) \\ \ddot{x}_2 = -\dot{x}_1 + \dot{x}_2(1 - x_1^2 - x_2^2) + x_2(-2x_1\dot{x}_1 - 2x_2\dot{x}_2) \end{array} \tag{44}$$

and after differentiating the accelerations with respect to time, the third derivatives $\dddot{x}_i$, are obtained

$$\begin{array}{l} \dddot{x}_1 = \dddot{x}_2 + \ddot{x}_1(1 - x_1^2 - x_2^2) + \dot{x}_1(-2x_1\dot{x}_1 - 2x_2\dot{x}_2) \\ \quad + \dot{x}_1(-2x_1\dot{x}_1 - 2x_2\dot{x}_2) + x_1(-2(\dot{x}_1^2 + x_1\ddot{x}_1) - 2(\dot{x}_2^2 + x_2\ddot{x}_2)) \\ \dddot{x}_2 = -\ddot{x}_1 + \ddot{x}_2(1 - x_1^2 - x_2^2) + \dot{x}_2(-2x_1\dot{x}_1 - 2x_2\dot{x}_2) \\ \quad + \dot{x}_2(-2x_1\dot{x}_1 - 2x_2\dot{x}_2) + x_2(-2(\dot{x}_1^2 + x_1\ddot{x}_1) - 2(\dot{x}_2^2 + x_2\ddot{x}_2)) \end{array} \tag{45}$$

Again, differentiating the third time the equations with respect to time, the fourth derivatives $\ddddot{x}_i$ are

$$\begin{array}{l} \ddddot{x}_1 = \dddot{x}_2 + \dddot{x}_1(1 - x_1^2 - x_2^2) + \ddot{x}_1(-2x_1\dot{x}_1 - 2x_2\dot{x}_2) \\ \quad + \ddot{x}_1(-2x_1\dot{x}_1 - 2x_2\dot{x}_2) + \dot{x}_1(-2(\dot{x}_1^2 + x_1\ddot{x}_1) - 2(\dot{x}_2^2 + x_2\ddot{x}_2)) \\ \quad + \ddot{x}_1(-2x_1\dot{x}_1 - 2x_2\dot{x}_2) \\ \quad + \dot{x}_1(-2(\dot{x}_1^2 + x_1\ddot{x}_1) - 2(\dot{x}_2^2 + x_2\ddot{x}_2)) \\ \quad + \dot{x}_1(-2(\dot{x}_1^2 + x_1\ddot{x}_1) - 2(\dot{x}_2^2 + x_2\ddot{x}_2)) \\ \quad + x_1(-2(2\dot{x}_1\ddot{x}_1 + \dot{x}_1\ddot{x}_1 + x_1\dddot{x}_1) - 2(2\dot{x}_2\ddot{x}_2 + \dot{x}_2\ddot{x}_2 + x_2\dddot{x}_2)) \\ \\ \ddddot{x}_2 = -\dddot{x}_1 + \dddot{x}_2(1 - x_1^2 - x_2^2) + \ddot{x}_1(-2x_1\dot{x}_1 - 2x_2\dot{x}_2) \\ \quad + \ddot{x}_1(-2x_1\dot{x}_1 - 2x_2\dot{x}_2) + \dot{x}_1(-2(\dot{x}_1^2 + x_1\ddot{x}_1) - 2(\dot{x}_2^2 + x_2\ddot{x}_2)) \\ \quad + \ddot{x}_1(-2x_1\dot{x}_1 - 2x_2\dot{x}_2) \\ \quad + \dot{x}_1(-2(\dot{x}_1^2 + x_1\ddot{x}_1) - 2(\dot{x}_2^2 + x_2\ddot{x}_2)) \\ \quad + \dot{x}_1(-2(\dot{x}_1^2 + x_1\ddot{x}_1) - 2(\dot{x}_2^2 + x_2\ddot{x}_2)) \\ \quad + x_1(-2(2\dot{x}_1\ddot{x}_1 + \dot{x}_1\ddot{x}_1 + x_1\dddot{x}_1) - 2(2\dot{x}_2\ddot{x}_2 + \dot{x}_2\ddot{x}_2 + x_2\dddot{x}_2)) \end{array} \tag{46}$$

These derivatives have been obtained analytically and form higher-order equivalent differential equations [9], which are used in the solution of the waveform of the nonlinear vectors, using the semi-analytical procedures considered in Section 2.4. Further higher order derivatives may be necessary to increase accuracy. Vector values of displacements, x_i, are then determined and updated recursively from the explicit Taylor series expansions.

$$x_{n+1} = x_n + \Delta t \dot{x}_n + \tfrac{\Delta t^2}{2!}\ddot{x}_n + \tfrac{\Delta t^3}{3!}\dddot{x}_n + ..., n = 0, 1, 2, 3, ... \tag{47}$$

where the exact values of velocity, acceleration and higher-order derivatives are evaluated from the higher-order equivalent differential equations.

3.4 Chaos: Lorenz equations

The three dimensional system derived by Lorenz demonstrates the phenomenon of chaos, and is given by

$$\begin{aligned} \dot{x} &= \sigma(y - x) \\ \dot{y} &= rx - y - xz \\ \dot{z} &= xy - bz \end{aligned} \tag{48}$$

where $\sigma, r, b > 0$, are parameters. σ is the Prandtl number, r is the Rayleigh number, and b is related to the aspect ratio of the rolls in the convection problem. This deterministic-looking system could have extremely erratic dynamics over a wide range of parameters, the solutions oscillate irregularly, never repeating, but always remaining in a bounded region of phase space. Lorenz looked at a model of convection rolls in the atmosphere.

In this article, the system is solved using semi-analytical procedures. The velocities $\dot{x}, \dot{y}, \dot{z}$, are obtained from the initial conditions x, y, z, given above. By differentiating the velocities with respect to time, the accelerations, $\ddot{x}_i$ are then obtained as follows: Differentiating the equations with respect to time, yields

$$\begin{aligned} \ddot{x} &= \sigma(\dot{y} - \dot{x}) \\ \ddot{y} &= r\dot{x} - \dot{y} - (\dot{x}z + x\dot{z}) \\ \ddot{z} &= \dot{x}y + x\dot{y} - b\dot{z} \end{aligned} \tag{49}$$

Repeated differentiation of the equations gives

$$\begin{aligned} \dddot{x} &= \sigma(\ddot{y} - \ddot{x}) \\ \dddot{y} &= r\ddot{x} - \ddot{y} - (\ddot{x}z + 2\dot{x}\dot{z} + x\ddot{z}) \\ \dddot{z} &= \ddot{x}y + 2\dot{x}\dot{y} + x\ddot{y} - b\ddot{z} \end{aligned}$$

$$\begin{aligned} \ddddot{x} &= \sigma(\dddot{y} - \dddot{x}) \\ \ddddot{y} &= r\dddot{x} - \dddot{y} - (\dddot{x}z + 3(\ddot{x}\dot{z} + \dot{x}\ddot{z}) + x\dddot{z}) \\ \ddddot{z} &= \dddot{x}y + 3(\ddot{x}\dot{y} + \dot{x}\ddot{y}) + x\dddot{y} - b\dddot{z} \end{aligned} \tag{50}$$

$$\begin{aligned} x^{(5)} &= \sigma(\dddot{y} - \ddddot{x}) \\ y^{(5)} &= r\ddddot{x} - \ddddot{y} - (\ddddot{x}z + \dddot{x}\dot{z} \\ &\quad + 3(\dddot{x}\ddot{z} + 2\ddot{x}\dot{z} + \dot{x}\dddot{z}) + \dot{x}\dddot{z} + x\ddddot{z}) \\ z^{(5)} &= \ddddot{x}y + \dddot{x}\dot{y} + 3(\dddot{x}\ddot{y} + 2\ddot{x}\dot{y} + \dot{x}\dddot{y}) \\ &\quad + \dot{x}\dddot{y} + x\ddddot{y} - b\ddddot{z} \end{aligned}$$

$$\begin{aligned} x^{(6)} &= \sigma(y^{(5)} - x^{(5)}) \\ y^{(6)} &= rx^{(5)} - y^{(5)} - (x^{(5)}z + \ddddot{x}\dot{z} \\ &\quad + \ddddot{x}\dot{z} + \dddot{x}\ddot{z} \\ &\quad + 3(\dddot{x}\dot{z} + \ddot{x}\ddot{z} \\ &\quad + 2(\dddot{x}\ddot{z} + \ddot{x}\dddot{z}) + \ddot{x}\dddot{z} + \dot{x}\ddddot{z}) \\ &\quad + \ddot{x}\ddot{z} + \dot{x}\dddot{z} + \dot{x}\dddot{z} + xz^{(5)}) \\ z^{(6)} &= x^{(5)}y + \ddddot{x}\dot{y} + \dddot{x}\ddot{y} + \ddot{x}\dddot{y} \\ &\quad + 3(\dddot{x}\dot{y} + \ddot{x}\ddot{y} \\ &\quad + 2(\ddot{x}\ddot{y} + \ddot{x}\dddot{y}) + \ddot{x}\dddot{y} + \dot{x}\ddddot{y}) \\ &\quad + \ddot{x}\dddot{y} + \dot{x}\ddot{y} + \dot{x}\dddot{y} + xy^{(5)} - bz^{(5)} \\ &.... \end{aligned} \tag{51}$$

The above derivatives have been obtained analytically and form higher-order equivalent differential equations [9] which are used in the solution of the waveform of the nonlinear vectors, using the semi-analytical procedures considered in Section 2.4. Further higher order derivatives may be necessary to increase accuracy. Vector values

of displacements, x_i, y_i, and z_i, are then determined and updated recursively from the explicit Taylor series expansions.

$$\begin{aligned} x_{n+1} &= x_n + \Delta t\dot{x}_n + \tfrac{\Delta t^2}{2!}\ddot{x}_n + \tfrac{\Delta t^3}{3!}\dddot{x}_n + ..., n = 0, 1, 2, 3, ... \\ y_{n+1} &= y_n + \Delta t\dot{y}_n + \tfrac{\Delta t^2}{2!}\ddot{y}_n + \tfrac{\Delta t^3}{3!}\dddot{y}_n + ..., n = 0, 1, 2, 3, ... \\ z_{n+1} &= z_n + \Delta t\dot{z}_n + \tfrac{\Delta t^2}{2!}\ddot{z}_n + \tfrac{\Delta t^3}{3!}\dddot{z}_n + ..., n = 0, 1, 2, 3, ... \end{aligned} \tag{52}$$

where the exact values of velocity, acceleration and higher-order derivatives are evaluated from the higher-order equivalent differential equations.

4 Results and discussions

First order, $\dot{x} = f(x, t)$, and second order, $\ddot{x} = f(\dot{x}, x, t)$, vector-valued differential equations have been solved. Explicit incremental solutions of nonlinear multiple-degree-of-freedom systems have been developed. Higher order equivalent differential equations were formulated and then subsequent values of vectors were updated using explicit Taylor series expansions. Clearly, as the time-step, $\Delta t \to 0$, the values of displacement and velocity are exact in the Taylor series expansions involving as many higher order derivatives as necessary.

Figure 9 shows a graph for the van der Pol equation with data: Velocity - displacement graph for: $\ddot{x} + \mu(x^2 - 1)\dot{x} + x = 0; x(0) = x_0, \dot{x}(0) = \dot{x}_0; \mu = 160$; for various initial conditions: $(0.5, 0.0)$; $(1.0, 100.0)$; $(1.0, -100.0)$; $(2.0, 100.0)$; $(2.0, -100.0)$; $(-1.0, 100.0)$; $(-1.0, -100.0)$; $(-2.0, 100.0)$; $(-2.0, -100.0)$; $\Delta t = 0.001$ seconds and having a limit cycle, using $\mu = 160$. Figure 10 shows a velocity - displacement graph, for the constants $\mu = 0, 1, 1.5, 2$. While the maximum displacement is $2(m)$, for the different constants, the maximum velocity for $\mu = 2$ is greater than that of $\mu = 1$, given by $\dot{x}_{max} = \frac{4}{3}\mu$. The bigger the constant, the greater the maximum velocity. For $\mu >> 1$, the value of period is, $\tau = \mu\frac{16}{9}$, which compares favourably with $\tau = \mu(3 - 2ln2) + 2\alpha\mu^{-0.333} + ...$, where $\alpha = 2.338$, as derived in Strogatz [12]. and therefore the corresponding natural frequency is, $\omega = \frac{1}{\mu}\frac{9\pi}{8}$. Figure 11 shows the corresponding displacement - time graph for $\mu = 0, 1, 2$.

Further developments consisted of closed-form solutions of the van der Pol equation, as shown in Table 1, with corresponding Figures (5), (6) and (7), showing, respectively, two graphs of velocity vs displacement and a graph of acceleration vs displacement. The curves are mostly enclosed inside the limit cycle determined using the semi-analytical procedures. The closed-form solutions show autonomus equations such that acceleration, $\ddot{x} = f(\dot{x}, x)$ and velocity, $\dot{x} = f(x)$, for $-\frac{4}{3}\mu < \dot{x} < \frac{4}{3}\mu$ and displacement, $-2 < x < 2$. What remains to be determined is the closed-form solution of, $x = f(t)$.

Table 3 shows profile data of functions in which self-time and total time spent in functions are compared. The displacement (s) truncation errors, E_s, are also indicated, taken from [7],[8], plus the type of algorithm, such as iterative (implicit) or incremental (explicit). The van der Pol constant used was $\mu = 160$, using a time-step of 0.001 seconds.

From Table 3, the fastest time was achieved by the Newmark equivalent scheme (maek1s2v) because of the least number of steps in the program. The second fast scheme (maek1s4v2022c) is the incremental scheme because it does not include iterative steps. The slowest scheme is the one-step five-value method (maek1s5v2nd3rd4th) which was a combined procedure including the second, third, fourth and fifth order equivalent differential equations. This scheme has the least truncation error in the table. The second slow scheme (maek1s4v2022) is the one-step four-value method which has the less truncation error than that of the Runge-Kutta method. Between one-step four-value and Runge-Kutta methods, the self-time and total time are not much different. The corresponding displacement vs time graph is shown in Figure 12. All the methods gave reasonably the same results, except the Newmark equivalent scheme whose plot indicate a slight phase lead. These results confirm those obtained in references [7] and [8].

Figure 13 shows a graph for the Duffing equation, taken from Thomson [16] wiith data: Velocity - displacement graph for: $\ddot{x} + \delta\dot{x} + \alpha x + \beta x^3 = \gamma cos(\omega t); x(0) = x_0, \dot{x}(0) = \dot{x}_0$. Initial conditions: $(0, 0), (-6, -6), (6, 6)$, and constants, $\delta = 0.4, \alpha = 1, \beta = 0.5, \gamma = 0.5, \omega = 0.5$. The steady-state conditions were reached after 1 cycle for various initial conditions, and Figure 14 shows a displacement - time graph for three initial conditions and the steady-state conditions were reached after 1 cycle. The results given in Thomson [16] are confirmed.

Figure 15 shows a graph for the nonlinear pendulum equation with data: Velocity - displacement graph for: $\ddot{\theta} + \frac{g}{l}sin(\theta) = 0$; $g = 9.81$ (m/s^2); length of pendulum: $l = 2$ (m); initial $\theta = \pi/8, 2\pi/8, 3\pi/8, 4\pi/8, 5\pi/8, 6\pi/8, 7\pi/8, 7.9\pi/8 \approx \pi$ (rad) for inner ring, initial $\theta = \pi/8$, whereas for outer ring, initial $\theta \approx \pi$; $\Delta t = 0.01$ seconds and having length $l = 2(m)$, for various initial angles of deflection from $\theta = \pi/8$ to a large $\theta \approx \pi$. Figure 16 shows a graph for the pendulum of length $l = 10(m)$. The maximum steady-state deflections for both cases are

Table 3: MATLAB profile data

File	Calls	Total time (seconds)	Self-time (seconds)	Error E_s	Iterative / Incremental
call	1	92.916	0.018		
maek1s5v2nd3rd4th	1	35.585	30.568	$-\frac{\Delta t^{11}}{11!}s^{(11)}(\zeta_s)$	Iterative
maek1s4v2022	1	27.126	2.792	$\frac{\Delta t^{9}}{9!}s^{(9)}(\zeta_s)$	Iterative
call-rkgen	1	11.227	0.013	$\frac{\Delta t^{5}}{5!}s^{(5)}(\zeta_s)$	Iterative
rkgen	1	11.181	10.255	$\frac{\Delta t^{5}}{5!}s^{(5)}(\zeta_s)$	Iterative
maek1s4v2022c	1	9.894	1.739	$\frac{\Delta t^{k}}{k!}s^{(k)}(\zeta_s)$	Incremental
maek1s2v (Newmark)	1	9.066	5.064	$\frac{\Delta t^{5}}{5!}s^{(5)}(\zeta_s)$	Iterative
maek1s4vb (4-value)	1	3.344	1.418	$\frac{\Delta t^{9}}{9!}s^{(9)}(\zeta_s)$	single iteration
maek1s5vb (5-value)	1	2.344	1.190	$-\frac{\Delta t^{11}}{11!}s^{(11)}(\zeta_s)$	single iteration
maek1s4vc	1	1.896	0.738	$\frac{\Delta t^{k}}{k!}s^{(k)}(\zeta_s)$	Incremental

Note:
Self time is the time spent in a function excluding anytime spent in child functions.
The time includes any overhead time resulting from the profiling process
The total time for the Runge-Kutta method is the total for call-rkgen and rkgen
The truncation error for the incremental scheme was of order $\mathrm{O}(\frac{\Delta t^{k})}{k!}s^{(k)}(\zeta_s), k = 10$
The last three lines show improved performances because of
minimising calls to external functions: using one function routine

practically the same whereas the maximum steady-state speed for the pendulum of length $l = 2(m)$ is higher than that of the pendulum of length $l = 10(m)$. The shorter pendulum swings faster than the longer pendulum for the same initial angles. Large initial angles resulted in nonlinear oscillatory motions of the pendulum, noticeable from the departure from a simple harmonic motion having a circular phase trajectory. This is also noticed in the graph of velocity vs time in Figure 17, which is not simple harmonic.

Figures 18 and 19 show graphs of velocity vs displacement for systems x_1 and x_2. The results of a nonlinear two-degrees-of-freedom first order differential equations taken from Meirovitch [15], are confirmed such that a limit cycle ended in a circle of radius 1, centred around $(0, 0)$, for various initial conditions. Higher order equivalent differential equations have been used to demonstrate how to extend from first and second order differential equations.

The examples for the Lorenz system have been left out in this article because the system requires a wide range of initial conditions to be tested together with a wide range of constants for the Prandtl and Rayleigh numbers to demonstrate the nature of chaos.

Figure 20 shows a graph of displacement vs time for a linear two-degrees-of-freedom system taken from Thomson [16]: $m_{11} = m_1 = 100, m_{12} = m_{21} = 0, m_{22} = m_2 = 25$; $b_{11} = b_{12} = b_{21} = b_{22} = 0$; $k_{11} = 54000, k_{12} = k_{21} = -18000, k_{22} = 18000$; $f_1 = 0, f_2 = 400$. The eigenvalues were found as, $\lambda_1 = 258.9$, with the corresponding fundamental natural frequency, $\omega_1 = 16.09$ rad/s, and $\lambda_2 = 1001.1$ with the corresponding natural frequency, $\omega_2 = 31.6$ rad/s. The results given in Thomson [16] are confirmed.

A finite element example is taken from Y. Wang et. al. [26], which was a multiple-degree-of-freedom mass-spring system with up to 1500 nonlinear springs, whose details are shown in Table 4. The system governing equations are given by those in Section 3.2, where each element of the spring matrix, K, is a function of displacement, u_i, and the system does not have damping. Figure 21 shows a graph of displacement vs time for a 10-dof system solved using a fixed time step of $\Delta t_0 = 1e-3(s)$. The CPU time was $2.197(s)$ for the duration of simulation of $10\pi(s)$ or 5 periodic cycles. Figure 22 shows a graph of displacement vs time for: a 100-dof system; given a prescribed $\Delta t_0 = 1e-02(s)$; with adaptive time stepping scheme used based on the radius of convergence and ratio test, $281.5945e-6 \leq \Delta t_n \leq 1e-3(s)$, CPU time, $254.616(s)$, whereas for fixed $\Delta t_0 = 1e-3(s)$, CPU time reduced to $69.094(s)$, for the same duration of simulation of $10\pi(s)$. Figure 23 shows a graph of displacement vs time for: a 200-dof system; given a prescribed $\Delta t_0 = 1e-02(s)$; with adaptive time stepping scheme used, $281.5945e-6 \leq \Delta t_n \leq 1e-3(s)$, CPU time, $965.138(s)$, whereas a CPU time of $258.764(s)$ for fixed $\Delta t_0 = 1e-3(s)$, for the same duration of simulation of $10\pi(s)$. Figure 24 shows a graph of displacement vs time for: a 500-dof system; prescribed $\Delta t_0 = 1e-02(s)$; with adaptive time stepping scheme

Table 4: Multiple-degree-of-freedom nonlinear mass-spring system

Mass (kg)	Spring (N/m)	Force (N)
$m_1 = 1$	$k_1 = k$	$f_1 = sin(t)$
m_2	k_2	$f_2 = sin(t)$
m_3	k_3	$f_3 = sin(t)$
...	...	...
m_n	k_n	$f_n = sin(t)$
	$k = 10^5$N/m	$\alpha = -2$

$m_i = 1$ kg, $\alpha = -2$, $k_i = k[1 + \alpha(u_i - u_{i-1})^2] \quad 2 \leq i \leq n$

used, $281.5945e-6 \leq \Delta t_n \leq 1e-3(s)$, CPU time, $5380.668(s)$, and for fixed $\Delta t_0 = 1e-03(s)$, CPU time of $1478.304(s)$, for the same duration of simulation of $10\pi(s)$. Figure 25 shows a graph of displacement vs time for a 1000-dof system solved using a fixed time step of $\Delta t_0 = 1e-3(s)$. The CPU time was $6485.748(s)$. While the CPU time is much greater than that of Y. Wang et. al. [26] having a time-step of $0.01(s)$, the graph is showing the same results, supporting the proof of concept for this incremental explicit method of solution which inevitably requires small time steps for both accuracy and stability. The theoretical truncation errors for displacement and velocity Taylor series recurrence equations used, were respectively, of order $O(\frac{\Delta t^N}{N!}x_{\zeta_s}^{(N)})$ and $O(\frac{\Delta t^{N-1}}{(N-1)!}x_{\zeta_v}^{(N)})$, with $N = 10$. The graphs revealed that for a small number of degrees of freedom, such as 10-dof, the response is sinusoidal, whereas for many degrees of freedom, for example, greater than 100-dof, the responses departed from the sinusoidal curves. For the examples solved here, the fixed prescribed time step resulted in less CPU time as shown in Table 5, mostly because, for the adaptable time stepping implemented, far smaller time steps were applied automatically, based on the radius of convergence and ratio test for optimal accuracy and stability.

Table 5: CPU time for a duration of 10π seconds or 5 periods

Degree of freedom	10	100	200	500	1000
Δt (s)	$1e-3$	$1e-3$	$1e-3$	$1e-3$	$1e-3$
Total time (s)	2.197	69.094	258.764	1478.304	6485.748

5 Conclusions

First order, $\dot{x} = f(x,t)$, and second order, $\ddot{x} = f(\dot{x},x,t)$, vector-valued nonlinear differential equations have been solved using explicit incremental semi-analytical solutions for nonlinear multiple-degree-of-freedom systems. Higher order equivalent differential equations were formulated and then subsequent values of vectors were updated using explicit Taylor series expansions. Clearly, as the time-step, $\Delta t \to 0$, the values of displacement and velocity are exact in the Taylor series expansions involving as many higher order derivatives as necessary.

Second order differential equations considered were, the van der Pol equation, Duffing equation and nonlinear equation for the pendulum. A first order equation, was a nonlinear two-degrees-of-freedom first order differential equation.

A linear system of two-degrees-of-freedom, taken from Thomson [16], was initially solved to illustrate how to extend the methods to deal with multiple-degrees-of-freedom systems using matrices and vectors, which are typically obtained in finite element methods, as shown in Table 4 with corresponding results shown in Figures 21, 22, 23, 24 and 25.

Further developments consisted of closed-form solutions of the van der Pol equation. The closed-form solutions showed autonomous equations such that acceleration, $\ddot{x} = f(\dot{x},x)$ and velocity, $\dot{x} = f(x)$, for $-\frac{4}{3}\mu < \dot{x} < \frac{4}{3}\mu$ and displacement, $-2 < x < 2$. What remains to be determined is the closed-form solution of, $x = f(t)$.

It is recommended that further applications of the semi-analytical procedures to time-dependent systems be extended to time-independent systems that are differentiable in terms of other independent variables, such as partial differential equations having many independent variables.

Declaration of competing interest

The author declares that there have been no known competing financial interests or personal relationships that could have appeared to influence the work reported in this paper.

Acknowledgements

This research did not receive any specific grant from funding agencies in the public, commercial, or not-for-profit sectors.

References

[1] Newmark, Nathan M. (1959), "A method of computation for structural dynamics", Journal of Engineering Mechanics, ASCE, 85 (EM3): 67-94.

[2] Hilber, H. M., Hughes, T. J. R., and Taylor, R. L. "Improved Numerical Dissipation for Time Integration Algorithms in Structural Dynamics", Earthquake Engineering and Structural Dynamics, 5 (1977), 283-292.

[3] Simo, J.C. and Taylor, R.L. "Consistent tangent operators for rate-independent elastoplasticity", Computer Methods in Applied Mechanics and Engineering, 48 (1985), 101-118, North-Holland.

[4] Wood, WL. Practical time-stepping schemes. Oxford, UK: Claredon Press; 1990.

[5] Bathe, K-J., Noh, G. "Insight into an implicit time integration scheme for structural dynamics". Computers and Structures, 98-99 (2012), 1-6.

[6] Zienkiewicz, O. C., Taylor, R. L. and Zhu, J. Z. The Finite Element Method: Its Basis and Fundamentals, 6th edition, Oxford, UK: Elsevier Butterworth-Heinemann; 2005.

[7] Kaunda, M. A. E. "Forward-backward-difference Time-integrating Schemes with Higher Order Derivatives for Non-linear Finite Element Analysis of Solids and Structures", Computers and Structures, 153, (2015), 1-18. http://doi.org/10.1016/j.compstruc.2015. 02.026.

[8] Kaunda M. A. E. "Improved numerical solutions of nonlinear oscillatory systems". Int J Numer Methods Eng. 2019;1-17. https://doi.org/10.1002/nme.6292.

[9] Smith, J. M. Mathematical Modelling and Digital Simulation for Engineers and Scientists, John Wiley and Sons Inc. 1977.

[10] Collatz, L. The numerical treatment of differential equations. 2nd printing of 3rd edition, Berlin, Germany: Springer Verlag/GMBH; 1966.

[11] Hildebrand, F. B. Introduction to numerical analysis, 2nd edition, Mineola, NY: Dover Publications, Inc.; 1974.

[12] Strogatz, Steven H. Nonlinear dynamics and chaos: with applications to physics, biology, chemistry, and engineering. Reading, MA: Perseus Books Publishers; 1994.

[13] La Salle, J., and Lefschetz, S. 1961. Stability by Liapunov's direct method with applications, RIAS, Inc. Baltimore, Maryland, Academic Press Inc.

[14] Irons, B.M. and Shrive, N.G. 1987. Numerical Methods in Engineering and Applied Science - Numbers are Fun, Ellis Horwood, Chichester.

[15] Meirovitch, L. Fundamentals of Vibrations, McGraw-Hill Higher Education, International Edition, 2001.

[16] Thomson, W.T. Theory of Vibrations with Applications, 2nd edition, George Allen and Unwin Ltd., 1983.

[17] Jordan, D. W. and Smith, P. Nonlinear ordinary differential equations: an introduction for scientists and engineers, 4th edition, New York, NY: Oxford University Press Inc.; 2007.

[18] Kreyszig, E. Advanced engineering mathematics, 10th edition, Wiley, 2011.

[19] E. V. Appleton, Proc. Cambridge Phil. Soc. 21 (1922), 231-4.

[20] B. van der Pol, Phil. Mag. 3 (1927), 65-80.

[21] On Non-Linear Differential Equations of the Second Order: II. The Equation $\ddot{y} + kf(y, \dot{y} + g(y, k) = p(t) = p_1(t) + kp_2(t); k > 0, f(y) \geqq 1$ Author(s): M. L. Cartwright and J. E. Littlewood Source: Annals of Mathematics, Apr., 1947, Second Series, Vol. 48, No. 2 (Apr., 1947), pp. 472-494 Published by: Mathematics Department, Princeton University Stable URL: https://www.jstor.org/stable/1969181.

[22] M. L. Cartwright, J. Instn Elect. Engrs, 95, Part m (1948), 88-96.

[23] M. L. Cartwright, Non-linear Vibrations: A Chapter in Mathematical History. Presidential Address to the Mathematical Association, January 3, 1952. edited by T. A. A. Broadbent, M.A. Royal Naval College, Greenwich, London, S.E. IO London G. Bell and Sons, Ltd., Portugal Street, Kingsway vol. XXXVI May, 1952 no. 316.

[24] Marios Tsatsos. "Theoretical and Numerical Study of the van der Pol equation", dissertation, Aristotle University of Thessaloniki School of Sciences, July 2006.

[25] Jean-Marc Ginoux. From Nonlinear Oscillations to Chaos Theory. The Foundations of Chaos Revisited: From Poincare to Recent Advancements, 2016. hal-01856968.

[26] Y. Wang, Tong Zhang, Xuelin Zhang, Shengwei Mei, Ningning Xie, Xiaodai Xue. "On an accurate A-posteriori error estimator and adaptive time stepping for the implicit and explicit composite time integration algorithms", Computers and Structures, 266, (2022). http://doi.org/10.1015/j.compstruc.2022.106789.

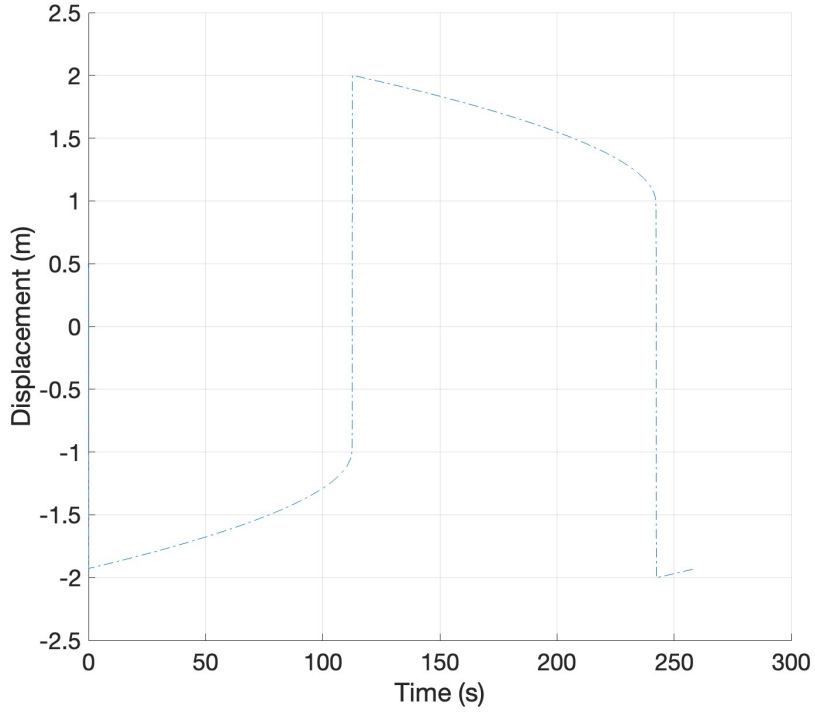

Figure 2: Displacement - time graph: Van der Pol equation: $\ddot{x}+\mu(x^2-1)\dot{x}+x=0; x(0)=x_0, \dot{x}(0)=\dot{x}_0; \mu=160;$ for initial conditions: $(0.5, 0.0)$; $\Delta t = 0.001$ seconds

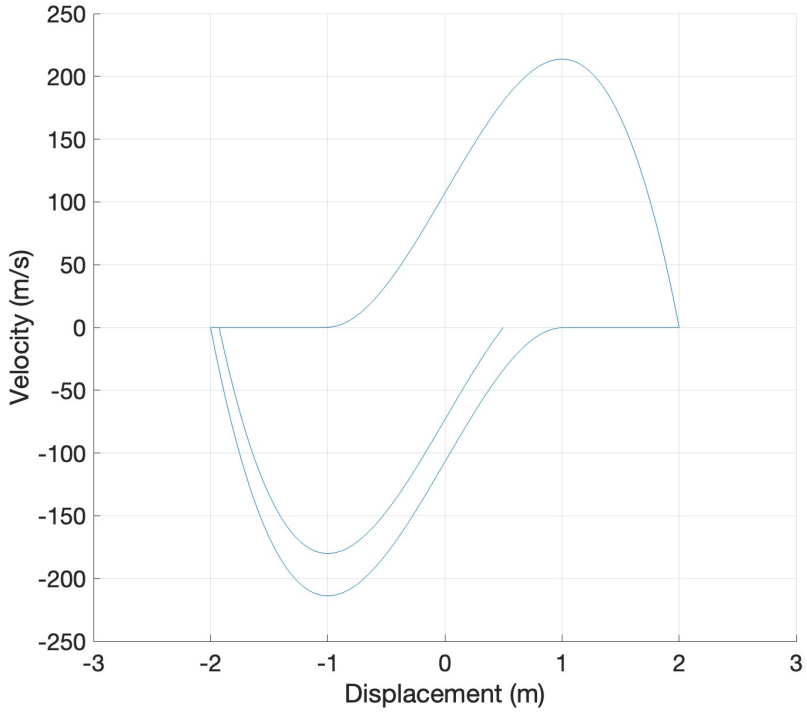

Figure 3: Velocity - displacement graph: Van der Pol equation: $\ddot{x}+\mu(x^2-1)\dot{x}+x=0; x(0)=x_0, \dot{x}(0)=\dot{x}_0; \mu=160;$ for initial conditions: $(0.5, 0.0)$; $\Delta t = 0.001$ seconds

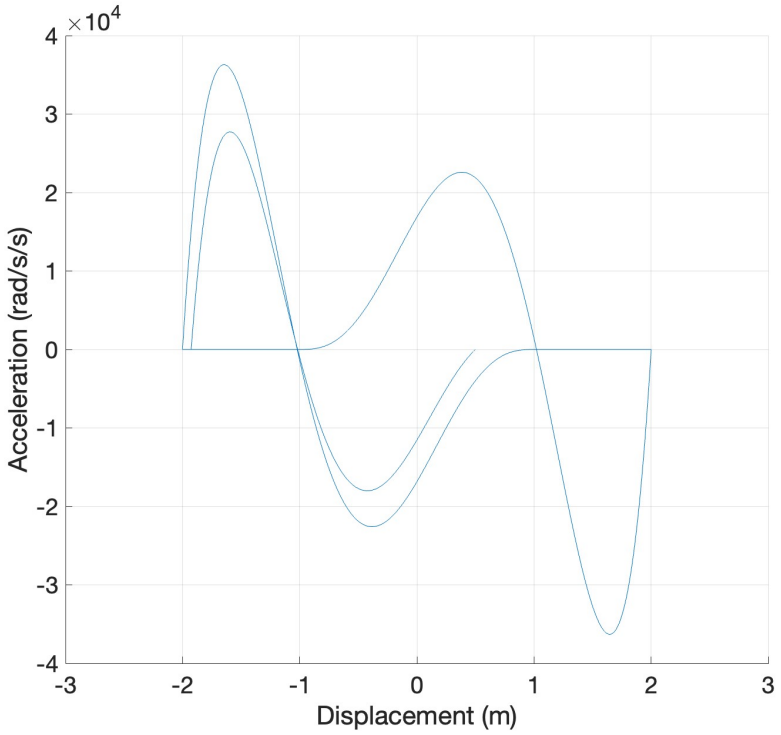

Figure 4: Acceleration - displacement graph: Van der Pol equation: $\ddot{x} + \mu(x^2 - 1)\dot{x} + x = 0; x(0) = x_0, \dot{x}(0) = \dot{x}_0; \mu = 160$; for initial conditions: $(0.5, 0.0)$; $\Delta t = 0.001$ seconds

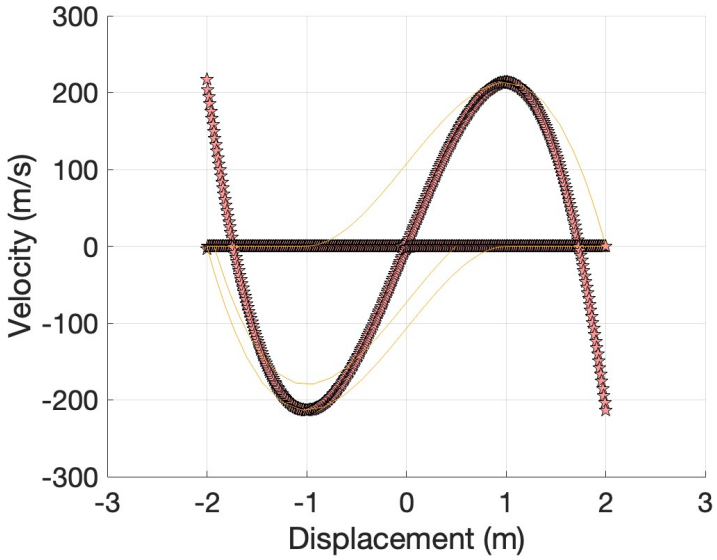

Figure 5: Velocity - displacement graph: Van der Pol equation: $\ddot{x} + \mu(x^2 - 1)\dot{x} + x = 0; x(0) = x_0, \dot{x}(0) = \dot{x}_0; \mu = 160$; for initial conditions: $(2.0, 0.0)$; Closed-form solution: $\frac{\dot{x}^2}{2} + \mu(\frac{x^3}{3} - x)\dot{x} + \frac{x^2}{2} + C = 0$; For $x = x_0, \dot{x} = \dot{x}_0, C = -[\frac{\dot{x}_0^2}{2} + \mu(\frac{x_0^3}{3} - x_0)\dot{x}_0 + \frac{x_0^2}{2}]$; Solve for the quadratic in $\dot{x}$ given any $-2 < x_t < 2$, and $\ddot{x} = -[\mu(x^2 - 1)\dot{x} + x]$

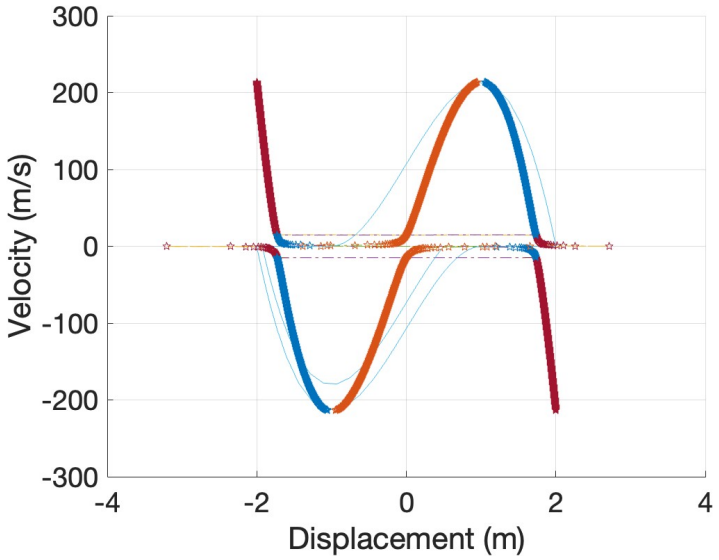

Figure 6: Velocity - displacement graph: Van der Pol equation: $\ddot{x}+\mu(x^2-1)\dot{x}+x=0; x(0)=x_0, \dot{x}(0)=\dot{x}_0; \mu=160$; for initial conditions: $(2.0, 0.0)$; Closed-form solution: For $x=x_0, \dot{x}=\dot{x}_0, C=-[\frac{\dot{x}_0^2}{2}+\mu(\frac{x_0^3}{3}-x_0)\dot{x}_0+\frac{x_0^2}{2}]$; $\mu\frac{x^3}{3}\dot{x}+\frac{x^2}{2}-\mu x\dot{x}+\frac{\dot{x}^2}{2}+C=0$; Solve for cubic in x given any $-\mu\frac{4}{3}<\dot{x}_t<\mu\frac{4}{3}$, and $\ddot{x}=-[\mu(x^2-1)\dot{x}+x]$

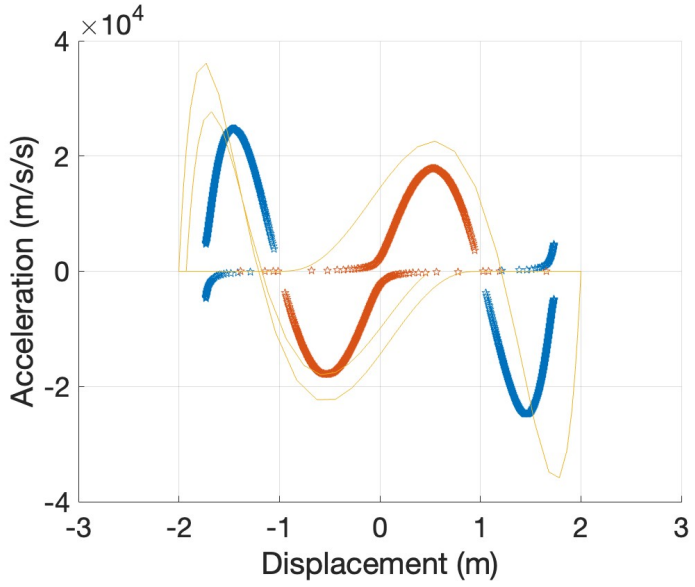

Figure 7: Acceleration - displacement graph: Van der Pol equation: $\ddot{x}+\mu(x^2-1)\dot{x}+x=0; x(0)=x_0, \dot{x}(0)=\dot{x}_0; \mu=160$; for initial conditions: $(2.0, 0.0)$; Closed-form solution: For $x=x_0, \dot{x}=\dot{x}_0, C=-[\frac{\dot{x}_0^2}{2}+\mu(\frac{x_0^3}{3}-x_0)\dot{x}_0+\frac{x_0^2}{2}]$; $\mu\frac{x^3}{3}\dot{x}+\frac{x^2}{2}-\mu x\dot{x}+\frac{\dot{x}^2}{2}+C=0$; Solve for cubic in x given any $-\mu\frac{4}{3}<\dot{x}_t<\mu\frac{4}{3}$, and $\ddot{x}=-[\mu(x^2-1)\dot{x}+x]$

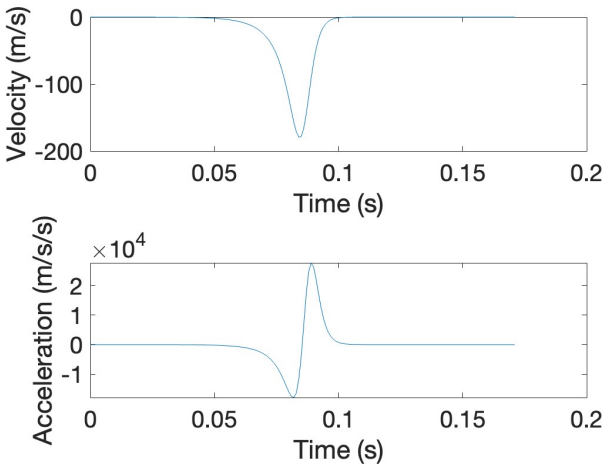

Figure 8: Velocity - time and Acceleration - time graphs: Van der Pol equation: $\ddot{x} + \mu(x^2 - 1)\dot{x} + x = 0 x(0) = x_0, \dot{x}(0) = \dot{x}_0; \mu = 160$, $\Delta t = 0.001$ seconds; showing peak velocity and peak acceleration and asymptotic curves

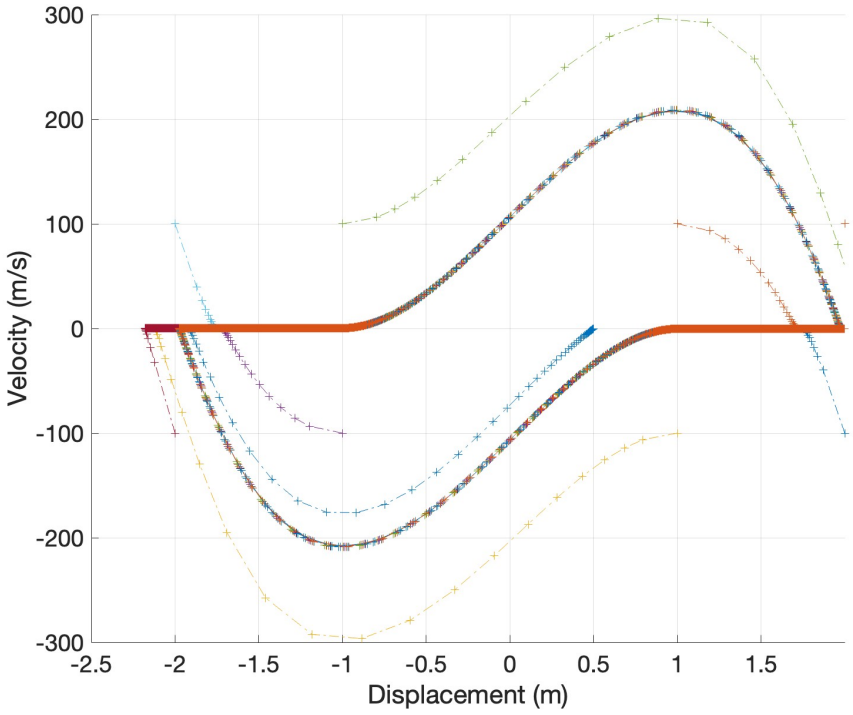

Figure 9: Velocity - displacement graph: Van der Pol equation: $\ddot{x} + \mu(x^2 - 1)\dot{x} + x = 0; x(0) = x_0, \dot{x}(0) = \dot{x}_0; \mu = 160$; for initial conditions: $(0.5, 0.0)$; $(1.0, 100.0)$; $(1.0, -100.0)$; $(2.0, 100.0)$; $(2.0, -100.0)$; $(-1.0, 100.0)$; $(-1.0, -100.0)$; $(-2.0, 100.0)$; $(-2.0, -100.0)$; $\Delta t = 0.001$ seconds

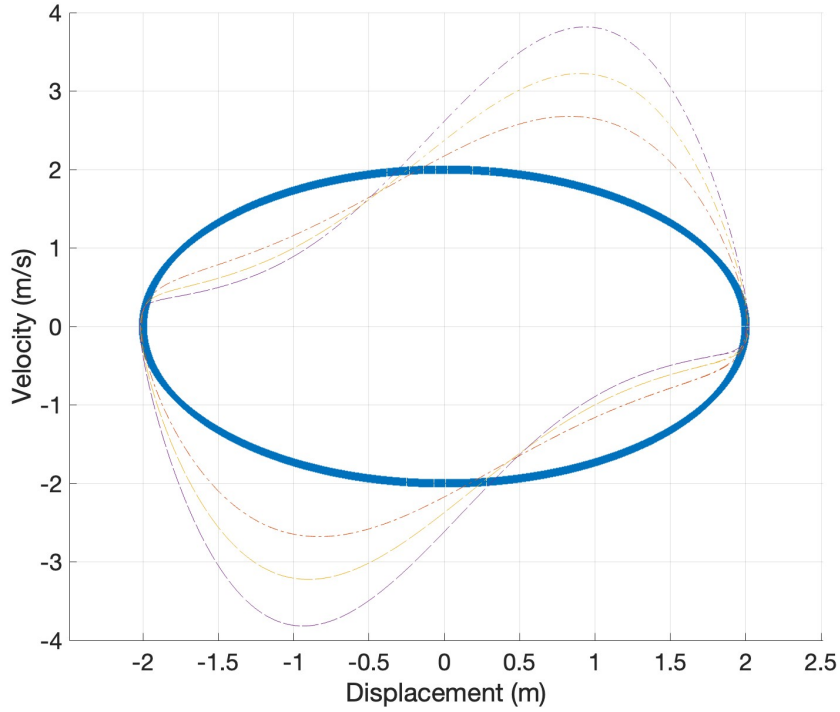

Figure 10: Velocity - displacement graph: Van der Pol equation: $\ddot{x} + \mu(x^2 - 1)\dot{x} + x = 0; x(0) = x_0, \dot{x}(0) = \dot{x}_0$; $\mu = 0, 1, 1.5, 2$ for inner ring $\mu = 0$, outer ring $\mu = 2$; initial conditions: $(2.0, 0.0)$; $\Delta t = 0.1$ seconds

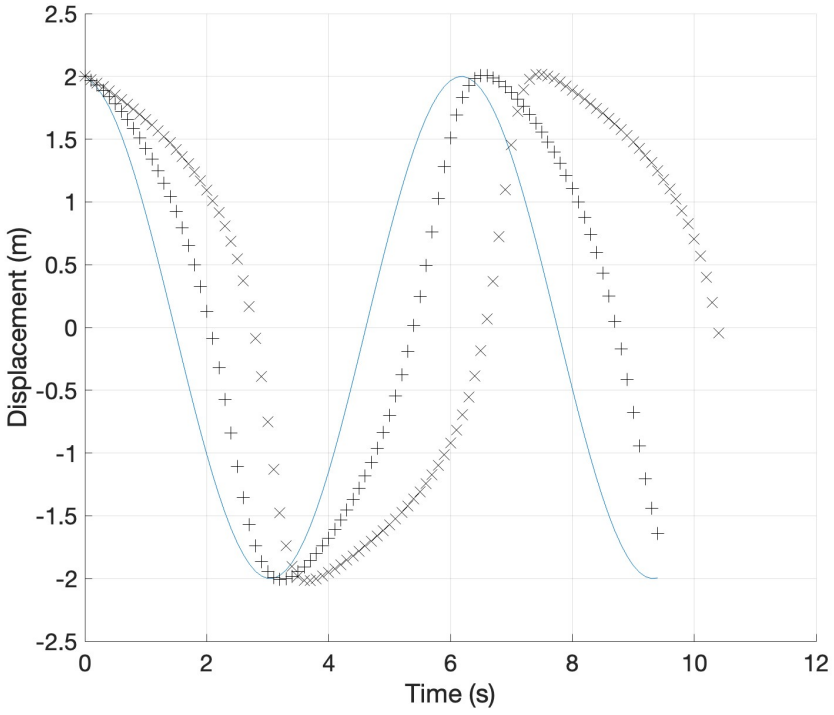

Figure 11: Displacement - time graph: Van der Pol equation: $\ddot{x} + \mu(x^2 - 1)\dot{x} + x = 0; x(0) = x_0, \dot{x}(0) = \dot{x}_0$; $\mu = 0$ " − "; $\mu = 1$ " + "; $\mu = 2$ "x"; initial conditions: $(2.0, 0.0)$; $\Delta t = 0.1$ seconds

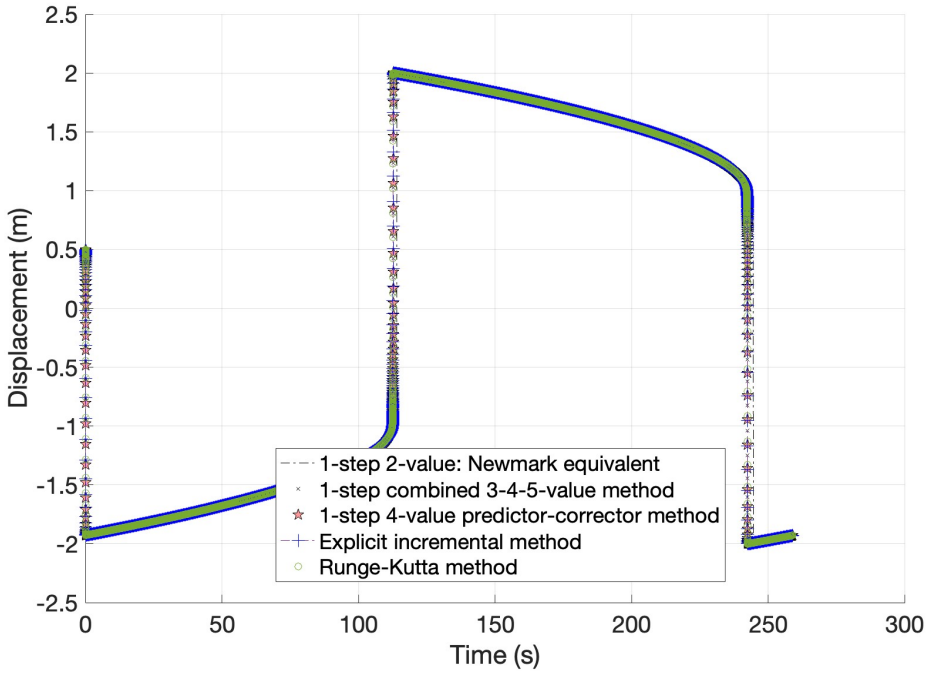

Figure 12: Displacement - time graph: Van der Pol equation: $\ddot{x} + \mu(x^2 - 1)\dot{x} + x = 0; x(0) = x_0, \dot{x}(0) = \dot{x}_0; \mu = 160$; initial conditions: $(0.5, 0.0)$; $\Delta t = 0.001$ seconds; plotted during profiling functions

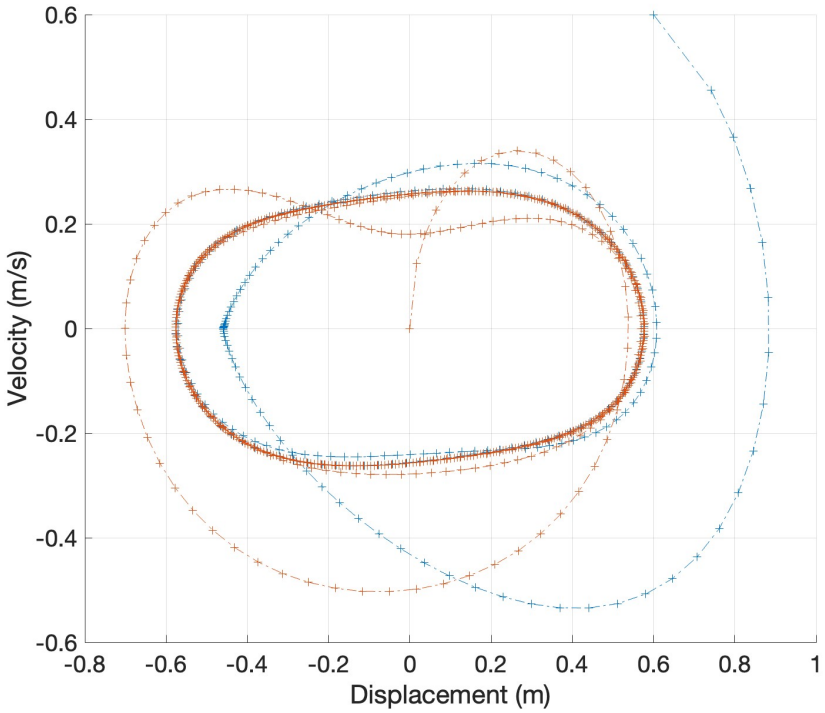

Figure 13: Velocity - displacement graph: Duffing equation: $\ddot{x} + \delta\dot{x} + \alpha x + \beta x^3 = \gamma cos(\omega t); x(0) = x_0, \dot{x}(0) = \dot{x}_0$. Initial conditions: $(0, 0), (-6, -6), (6, 6)$, and constants, $\delta = 0.4, \alpha = 1, \beta = 0.5, \gamma = 0.5, \omega = 0.5$; steady-state conditions reached after 1 cycle

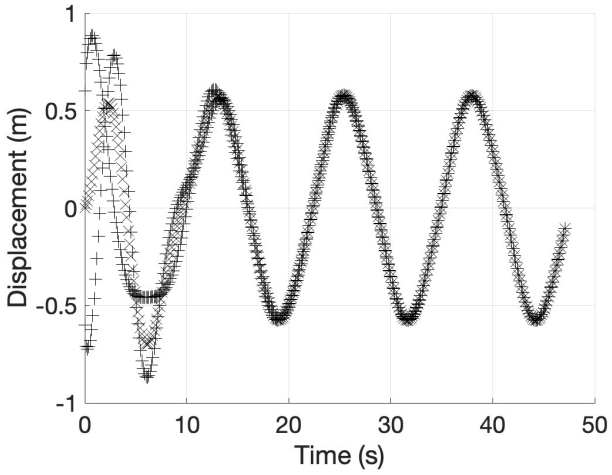

Figure 14: Displacement - time graph: Duffing equation: $\ddot{x} + \delta\dot{x} + \alpha x + \beta x^3 = \gamma cos(\omega t); x(0) = x_0, \dot{x}(0) = \dot{x}_0$. Initial conditions: $(0, 0), (-6, -6), (6, 6)$, and constants, $\delta = 0.4, \alpha = 1, \beta = 0.5, \gamma = 0.5, \omega = 0.5$; steady-state conditions reached after 1 cycle

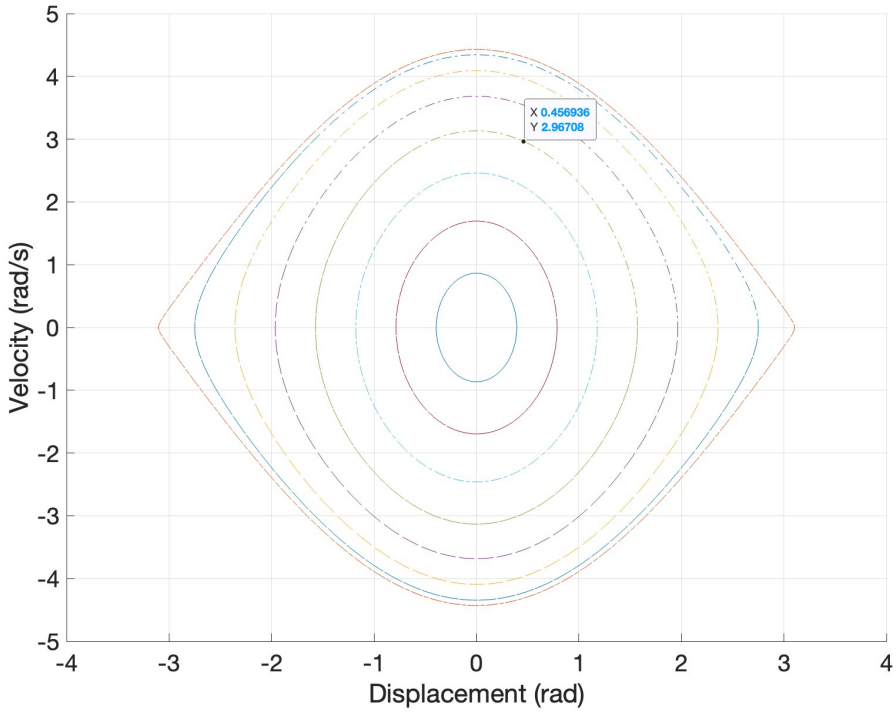

Figure 15: Velocity - displacement graph: Pendulum equation: $\ddot{\theta} + \frac{g}{l} sin(\theta) = 0$; $g = 9.81$ (m/s^2); length of pendulum: $l = 2$ (m); initial $\theta = \pi/8, 2\pi/8, 3\pi/8, 4\pi/8, 5\pi/8, 6\pi/8, 7\pi/8, 7.9\pi/8 \approx \pi$ (rad) for inner ring, initial $\theta = \pi/8$, outer ring, initial $\theta \approx \pi$; $\Delta t = 0.01$ seconds

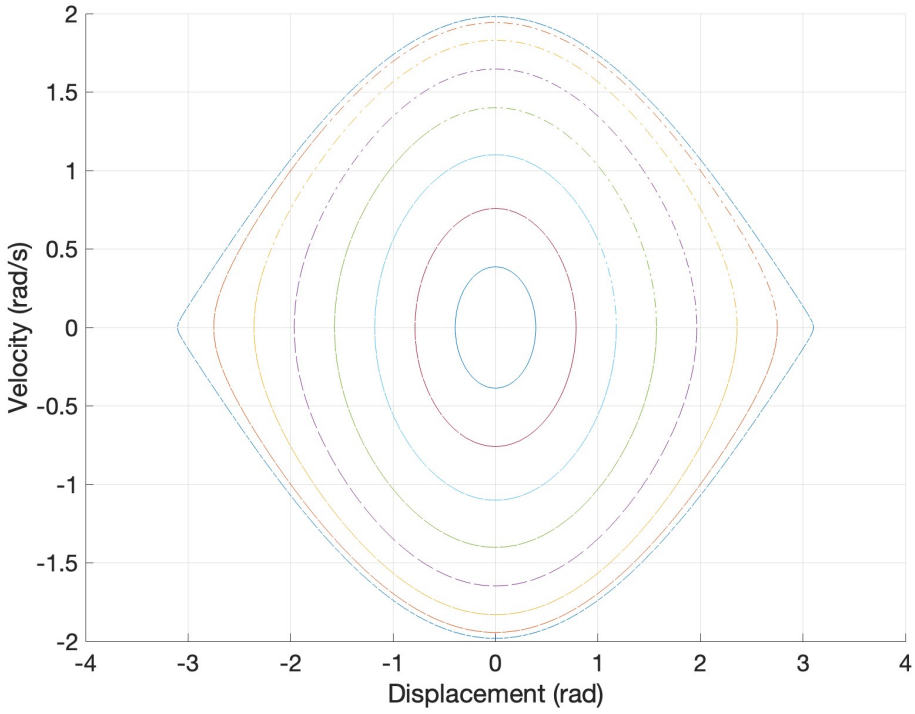

Figure 16: Velocity - displacement graph: Pendulum equation: $\ddot{\theta} + \frac{g}{l} sin(\theta) = 0$; $g = 9.81$ (m/s^2); length of pendulum: $l = 10$ (m); initial $\theta = \pi/8, 2\pi/8, 3\pi/8, 4\pi/8, 5\pi/8, 6\pi/8, 7\pi/8, 7.9\pi/8 \approx \pi$ (rad) for inner ring, initial $\theta = \pi/8$, outer ring, initial $\theta \approx \pi$; $\Delta t = 0.01$ seconds

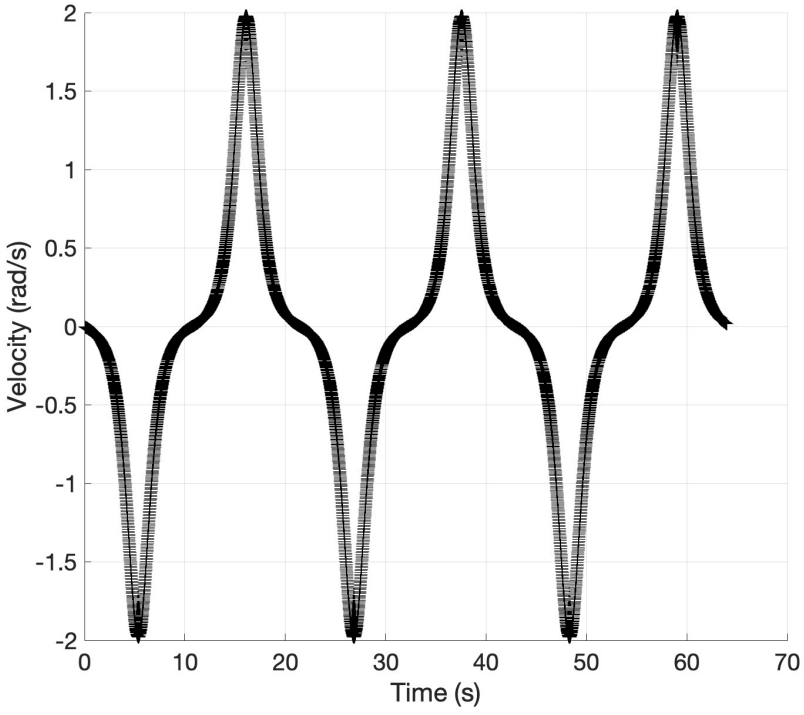

Figure 17: Velocity - time graph: Pendulum equation: $\ddot{\theta} + \frac{g}{l} sin(\theta) = 0$; $g = 9.81$ (m/s^2); length of pendulum: $l = 10$ (m); initial $\theta = 7.9\pi/8 \approx \pi$ (rad); $\Delta t = 0.01$ seconds

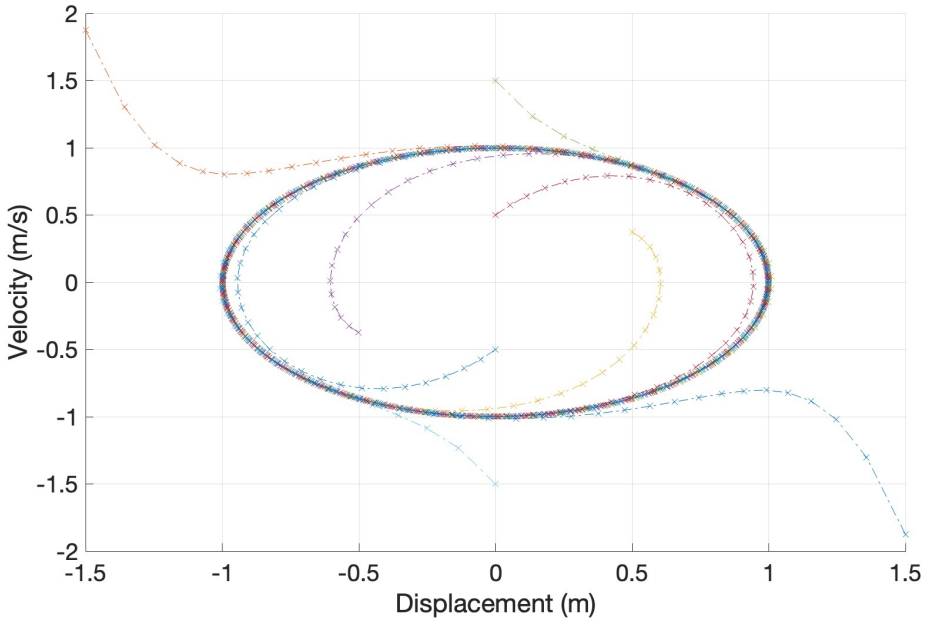

Figure 18: Graph of velocity vs displacement: System-x_1; initial conditions: (1.5,0),(-1.5,0),(0.5,0),(-0.5,0), (0,1.5),(0,-1.5),(0,0.5),(0,-0.5); $\Delta t = 0.1, 0.01, 0.001, 0.0001$ seconds, gave same limit cycles.

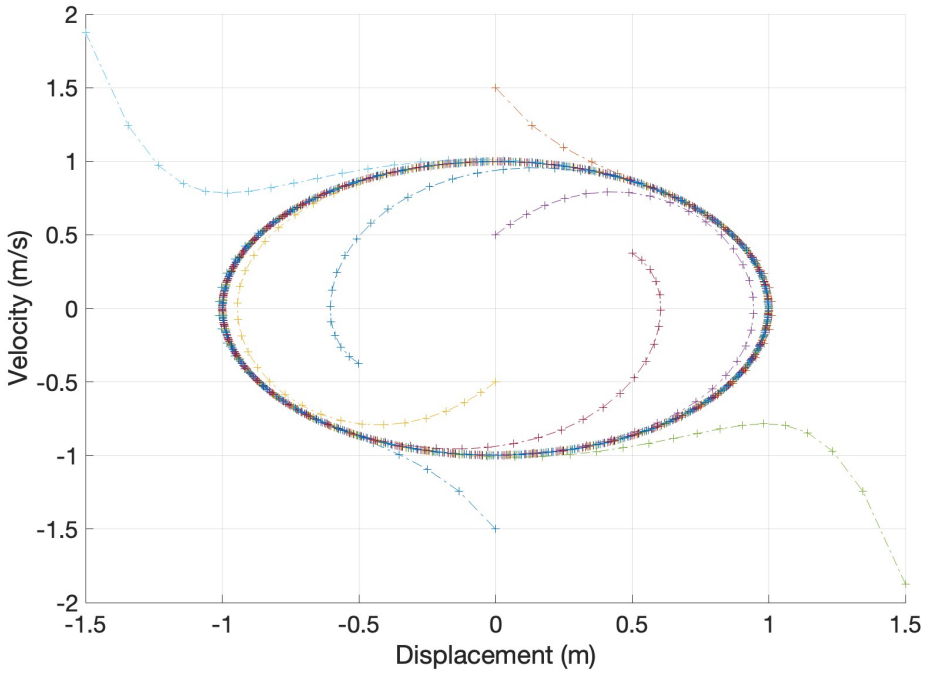

Figure 19: Graph of velocity vs displacement: System-x_2; initial conditions: (1.5,0),(-1.5,0),(0.5,0),(-0.5,0), (0,1.5),(0,-1.5),(0,0.5),(0,-0.5); $\Delta t = 0.1, 0.01, 0.001, 0.0001$ seconds, gave same limit cycles.

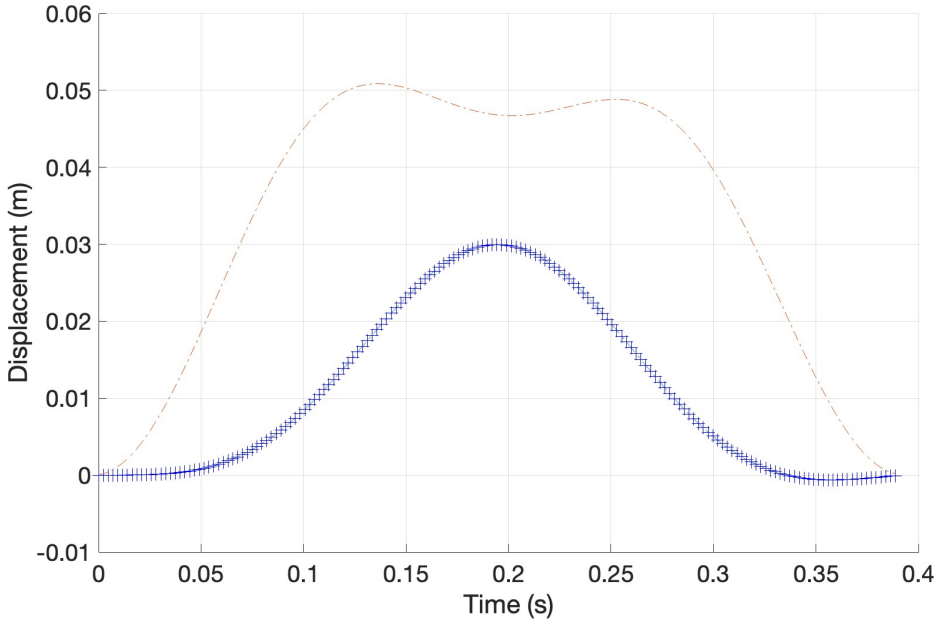

Figure 20: Graph of displacement vs time: 2-dof system; $x(0) = 0$, $\dot{x}(0) = 0$, $\Delta t = 2.3416e - 06(s)$; 2-dof: $m_{11} = 100, m_{12} = m_{21} = 0, m_{22} = 25$; $b_{11} = b_{12} = b_{21} = b_{22} = 0$; $k_{11} = 54000, k_{12} = k_{21} = -18000, k_{22} = 18000$; $f_1 = 0, f_2 = 400$

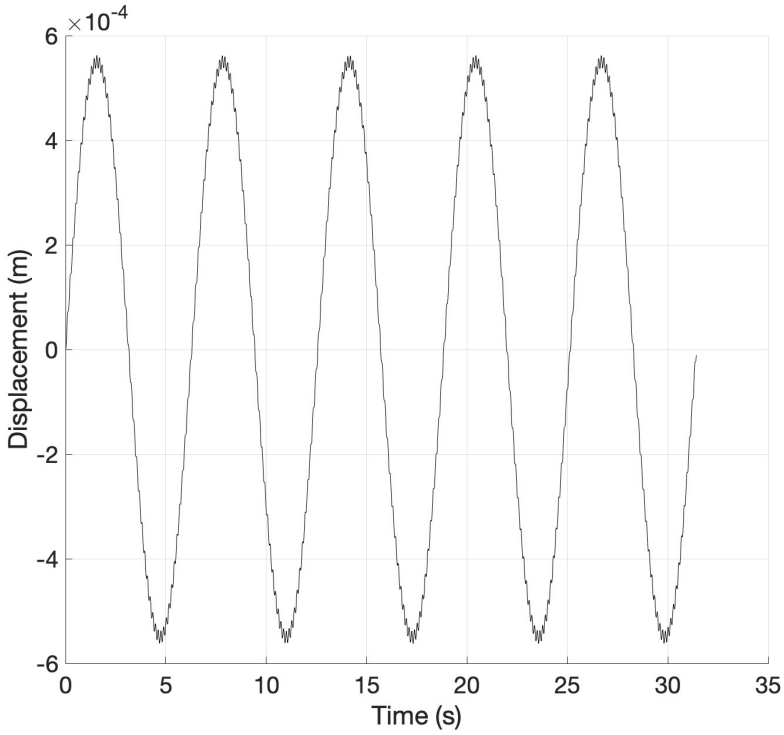

Figure 21: Graph of displacement vs time: 10-dof system; fixed $\Delta t_0 = 1e - 03(s)$; CPU time, $2.197(s)$, duration of simulation, $10\pi(s)$

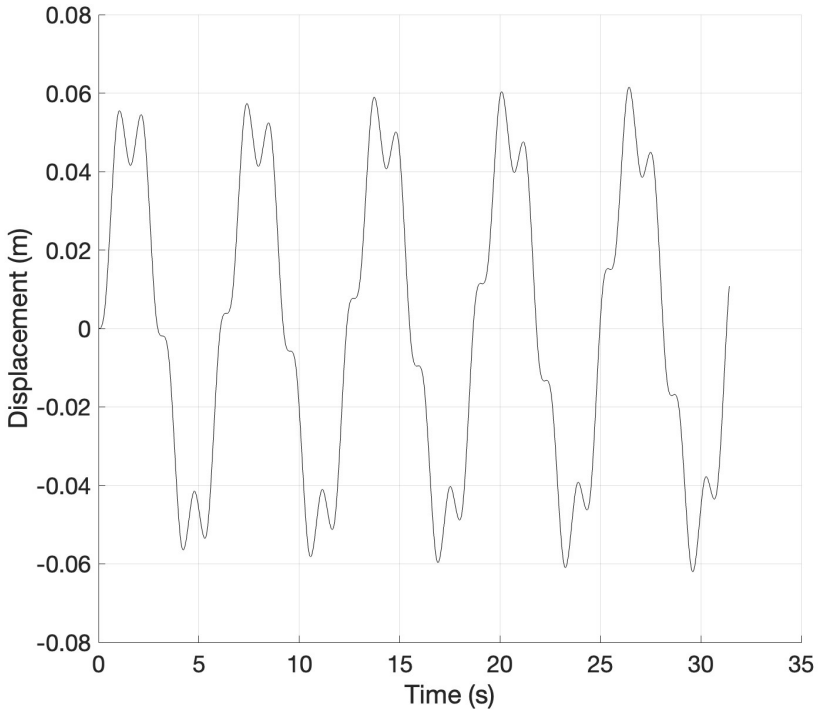

Figure 22: Graph of displacement vs time: 100-dof system; $\Delta t_0 = 1e-02(s)$; with adaptive time stepping scheme used, $281.5945e-6 \leq \Delta t_n \leq 1e-3(s)$, CPU time, $254.616(s)$; fixed $\Delta t_0 = 1e-3(s)$, CPU time, $69.094(s)$, duration of simulation, $10\pi(s)$

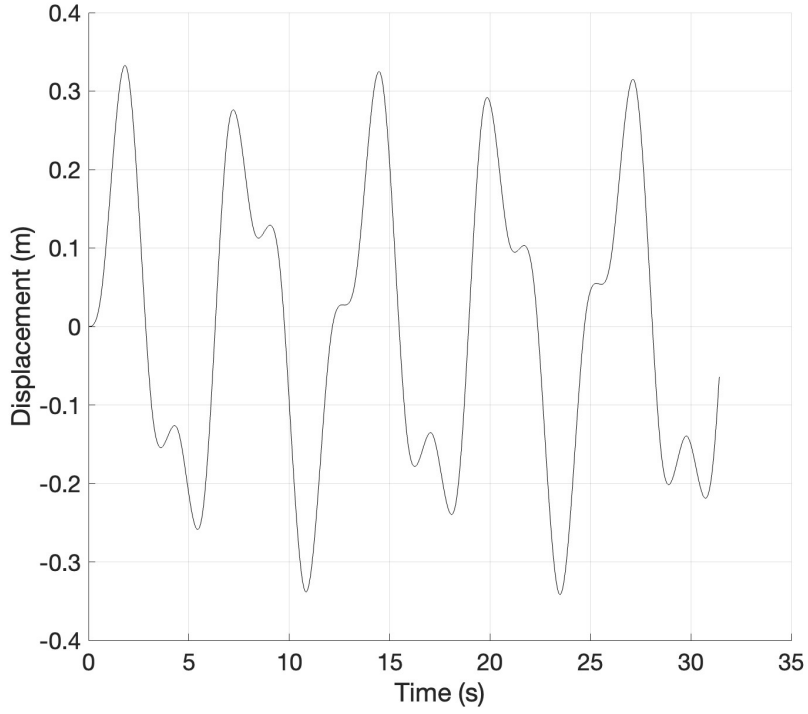

Figure 23: Graph of displacement vs time: 200-dof system; $\Delta t_0 = 1e-02(s)$; with adaptive time stepping scheme used, $281.5945e-6 \leq \Delta t_n \leq 1e-3(s)$, CPU time, $965.138(s)$; fixed $\Delta t_0 = 1e-3(s)$, CPU time, $258.764(s)$duration of simulation, $10\pi(s)$

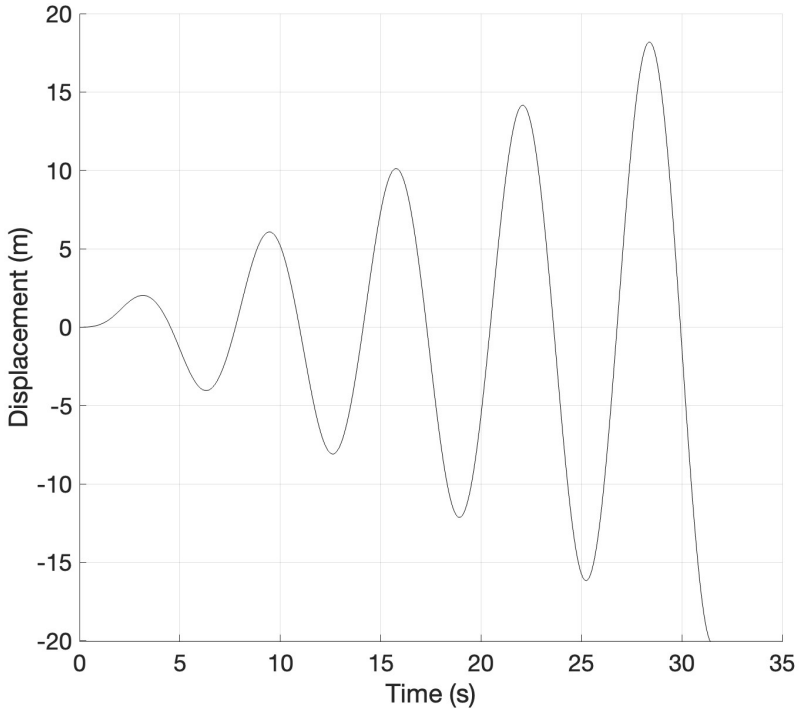

Figure 24: Graph of displacement vs time: 500-dof system; $\Delta t_0 = 1e-02(s)$; with adaptive time stepping scheme used, $281.5945e-6 \leq \Delta t_n \leq 1e-3(s)$, CPU time, $5380.668(s)$, fixed $\Delta t_0 = 1e-03(s)$, CPU time, $1478.304(s)$, duration of simulation, $10\pi(s)$

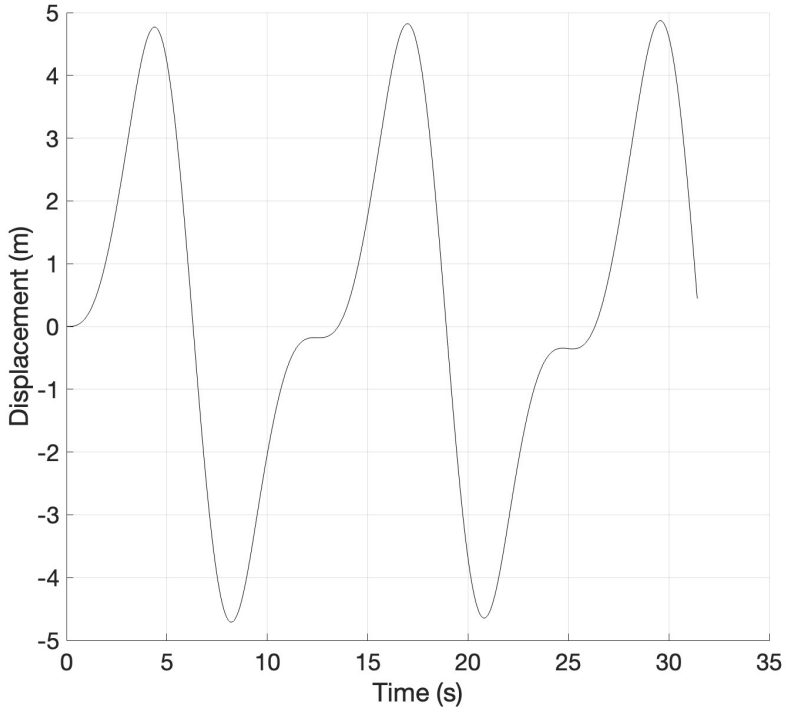

Figure 25: Graph of displacement vs time: 1000-dof system; fixed $\Delta t_0 = 1e-03(s)$; CPU time, $6485.748(s)$, duration of simulation, $10\pi(s)$